VYSOKÉ UČENÍ TECHNICKÉ V BRNĚ

BRNO UNIVERSITY OF TECHNOLOGY

FAKULTA STROJNÍHO INŽENÝRSTVÍ

ÚSTAV MECHANIKY TĚLES, MECHATRONIKY A BIOMECHANIKY

FACULTY OF MECHANICAL ENGINEERING

INSTITUTE OF SOLID MECHANICS, MECHATRONICS AND BIOMECHANICS

DESIGN AND IMPLEMENTATION OF TESTING DEVICE FOR GONIO MECHANISMS

NÁVRH A REALIZACE ZAŘÍZENÍ PRO TESTOVÁNÍ GONIOVÝCH MECHANISMŮ

DIPLOMOVÁ PRÁCE

MASTER'S THESIS

AUTOR PRÁCE — Bc. FRANTIŠEK VAŠKE

AUTHOR

VEDOUCÍ PRÁCE — doc. Ing. RADEK VLACH, Ph.D.

SUPERVISOR

BRNO 2012

Vysoké učení technické v Brně, Fakulta strojního inženýrství

Ústav mechaniky těles, mechatroniky a biomechaniky
Akademický rok: 2011/2012

ZADÁNÍ DIPLOMOVÉ PRÁCE

student(ka): Bc. František Vaške

který/která studuje v **magisterském navazujícím studijním programu**

obor: **Mechatronika (3906T001)**

Ředitel ústavu Vám v souladu se zákonem č.111/1998 o vysokých školách a se Studijním a zkušebním řádem VUT v Brně určuje následující téma diplomové práce:

Návrh a realizace zařízení pro testování goniových mechanismů

v anglickém jazyce:

Design and implementation of testing device for gonio mechanisms

Stručná charakteristika problematiky úkolu:

Práce se bude zabývat návrhem a implementací testovacího zařízení pro goniové mechanismy. Testovací zařízení má za cíl kontrolní měření přesnosti mechanismu ve dvou osách a její následné vyhodnocení
Na základě archivních záznamů o závadách mechanismu bude úkolem změna konstrukce goniového mechanismu s cílem eliminovat jeho současné nedostatky a zajistit větší robustnost konstrukce mechanismu.

Cíle diplomové práce:

1) Proveďte rešeršní studii pohybů goniového mechanismu a metod měření potřebných veličin.
2) Navrhněte koncepci testovacího zařízení s využitím současných měřicích prostředků. Vytvořte jednoduché grafické uživatelské rozhraní pro ovládání testovacího zařízení pomocí PC.
3) Proveďte statistické vyhodnocení přesnosti chodu mechanismu.
4) Vytvořte přehled současných problémů goniového mechanismu.
5) Na základě získaných dat navrhněte a otestujte změny v konstrukci goniového mechanismu.

Seznam odborné literatury:

1. Marsh, Eric R.: Precision spindle metrology, Destech Publications, Inc.
2. Wilson, Jon S.: Sensor technology handbook, Elsevier, Inc.
3. Karpíšek, Z.: Matematika IV: statistika a pravděpodobnost, CERM
4. Sydenham P.:Handbook of measurement science, Composition house

Vedoucí diplomové práce: doc. Ing. Radek Vlach, Ph.D.

Termín odevzdání diplomové práce je stanoven časovým plánem akademického roku 2011/2012.

V Brně, dne 21.11.2011

L.S.

_____	_____
prof. Ing. Jindřich Petruška, CSc.	prof. RNDr. Miroslav Doupovec, CSc., dr. h. c.
Ředitel ústavu	Děkan fakulty

Abstract

This thesis deals with design and implementation of testing device for measurement of motion repeatability of a goniometer mechanism, also with measurement of the mechanism's motion characteristics and evaluation of data measured. It also implements some design changes to the mechanism and evaluates parameters of a prototype.

Abstrakt

Tato práce se zabývá návrhem a implementací zařízení na měření opakovatelnosti pohybu goniového mechanismu, dále měřením pohybových vlastností mechanismu a vyhodnocením naměřených dat. Popisuje navrhnuté a zavedené změny na mechanismu a vyhodnocuje vlastnosti prototypu.

Thanks

I would like to thank to everyone who helped me with advice and guidance.

Declaration on word of honour

I statutory declare, that I wrote this paper by myself with usage of stated literature and under supervision of my instructor.

František Vaške, Brno, 2012

Contents

List of abbreviations

abbr	meaning
SEM	Scanning electron microscope
TEM	Transmission electron microscope
CCD	Charge coupled device
X,Y,Z,R,T	Motion axes
DC	Direct current
MPC	Microscope PC
SPC	Support PC
PWM	Pulse width modulation
COM	Component object model
dll	Dynamic link library
VI	Virtual instrument
RS232	Serial communication protocol
PTP	Point to point
BOM	Bill of material
MCU	Motion control unit
FEG	Field emission gun

1. Introduction

This thesis deals with the problem of movement repeatability measurement of a goniometer mechanism, problems related to precision of its movement and their particular solutions.

The mechanism considered here is a sample positioning stage for scanning electron microscope made by FEI Company. There are extreme requirements for accuracy of the mechanism movement and series of tests are executed to ensure that. One of them is the repeatability test. The aim of the study is to design a low-cost device for this measurement. Purpose of such tool is to provide means of measurement to a third party stage manufacturer so he could analyse a stage before delivering it to FEI. Design of the device should be preceded by literature search considering possible conceptions of measurement and their advantages and disadvantages.

This thesis should also provide summary of current issues related to stage's behaviour and parameters. Based on this survey, weak spots of the stage should be identified and design changes made, tested and evaluated in attempt to solve the most significant problems.

Picture1 - Quanta series SEM, FEI company [1]

2.Issue overview

2.1. Electron microscope

The principle of an electron microscope is the very same as of a classic optical one. However, instead of visible light and glass lenses there is electron beam and lenses are formed by electromagnetic field. The reason for using electrons instead of visible light is simple – resolution of an optical microscope is limited by two factors: wavelength of illumination (it would be 400 nm for violet light) and numeric aperture of an objective (today best about 1.4). Rayleigh equation for resolution says [2]:

$$d = 1.22\left(\frac{l}{2NA}\right) = 1.22\left(\frac{400nm}{2 \cdot 1.4}\right) \doteq 174nm \quad (1)$$

Where l is wavelength, NA is numeric aperture and d is distance between two adjacent particles.

Electrons accelerated by 300kV (commonly used voltage for TEM, 30kV for SEM) have wavelength approximately 0.002 nm and microscopes using them can reach sub-angstrom (0.1nm) resolution.

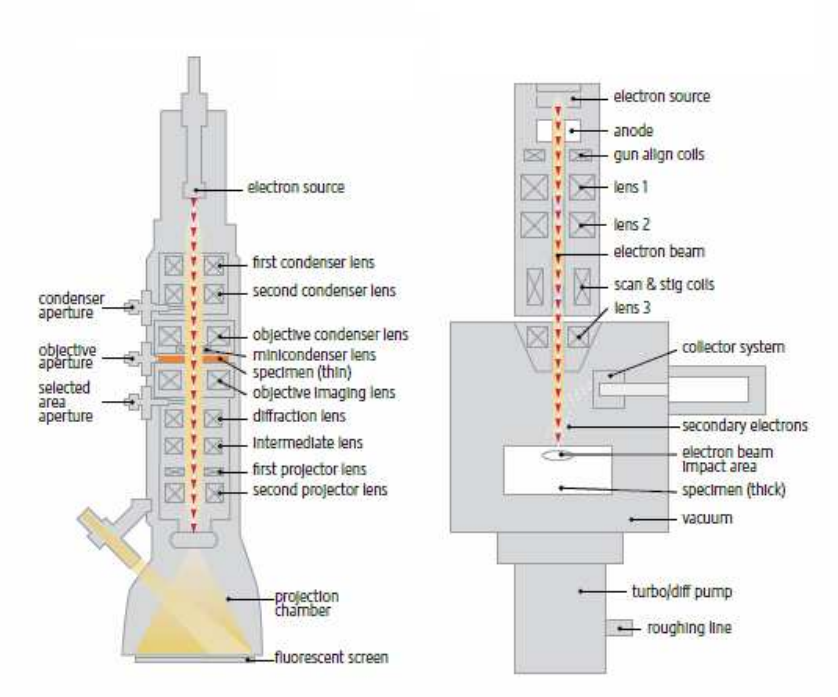

Picture 2 - TEM and SEM principle [3]

The most of electron microscopes can be classified as one of two basic types: Transmission Electron Microscope (TEM) and Scanning Electron Microscope (SEM). Both of them operate under vacuum. The main difference between them is that in TEM an electron beam shines through a very thin sample and displays its image on a fluorescent plane (or CCD today) while a SEM scans surface of a sample point-by-point with a fine focused beam and backscattered or secondary electrons are detected and an image is reconstructed in special software afterwards.

Transmission microscopes achieve higher resolution but have very high demands on a sample and due to much higher energy of electrons used they damage the sample very fast. On the other hand, it is possible to put wide range of samples into SEM, like sensitive (e.g. biological) samples or quite the opposite samples which need to be very hot or cold.

However, from the point of view of this thesis there is another very important thing. The nature of a SEM construction (Picture 2) and the fact that a sample can be relatively big leads to need for a very precise positioning system – a stage.

2.2. Stage

A microscope stage is a mechanism with five degrees of freedom corresponding with translation in axes X, Y, Z, rotation around R and rotation around axis T. This last axis is in the plane defined by X and Z and is parallel to X (see Picture 5).

There are various kinds of stages using several principles of actuation. The most precise types are driven by piezomotors which are placed directly on the axis they operate and when they are complemented with diffraction linear encoders a stage can move with the smallest step of 10nm and precision less than 100nm [1]. However, this particular solution is very expensive and because of that ordinary DC motors with rotary encoders are used for midrange and low cost microscopes.

The 50mm DC stage (Picture 3) used in Quanta and Inspect series SEMs made by FEI company is a basic model based on design from 1980's (50mm stands for its movement range in XY plane). The original model was positioned only manually by knobs with a micrometric screw on the front of the vacuum chamber door.

The only functional innovation implemented was that DC servos were added to the door (Picture 4). This solution made computer control possible, but motors (and encoders more importantly) are too far from the stage itself so the position must be sometimes adjusted manually according to microscope's image. The 50mm stages are manufactured in two versions – with manual or motorised tilt axis. They are mounted

into different microscope configurations. Motorised tilt is used for microscopes which have also an ion gun in addition to an electron column. Ion columns are attached to a chamber in 52° angle so that's why a sample has to be tilted precisely between two planes.

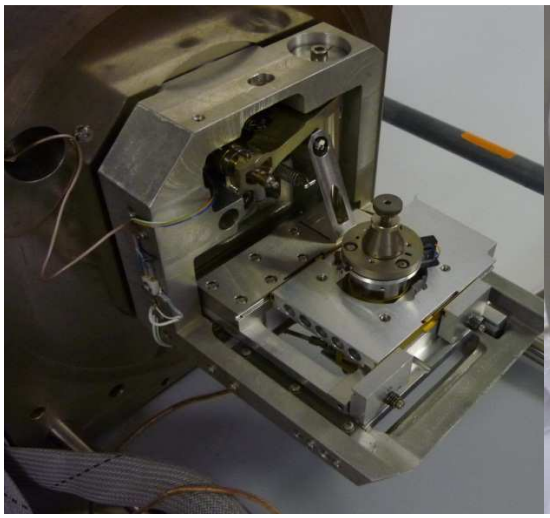

Picture 3 - 50mm C stage

Picture 4 - DC servos

There is a goniometer mechanism mentioned in the assignment of the thesis, it is another name for a stage which can rotate around an eucentric axis.

In this case the eucentric axis is the rotation axis of T (for tilt) axis. When a sample is placed in such height that it lies on the eucentric axis it can be traversed and tilted at will without need of refocusing the electron beam.

2.3. Stage's mechanics

Only mechanical parts which are related to planar movements are described here. In the Picture 5 there is a 50mm stage while looking from inside the chamber. The motion of X and Y motors is transferred through chamber door by flexible couplings and shafts. Then by another couplings to prestressed threaded rods (6) which transform rotation to linear motion. The right-angled arm (8) moves along X threaded rod and moves the X slide (1) which carries Y slide (2) along with RZ unit (12) and sample holder (5). The Y threaded rod rotates lever (7) around vertical axis, this rotation is then transmitted to Y slide linear motion by snub pulley (9). It consists of set of ball bearings mounted to a small lever which is pushed to the sides of a groove by a wounded spring (details in 4.2.3).

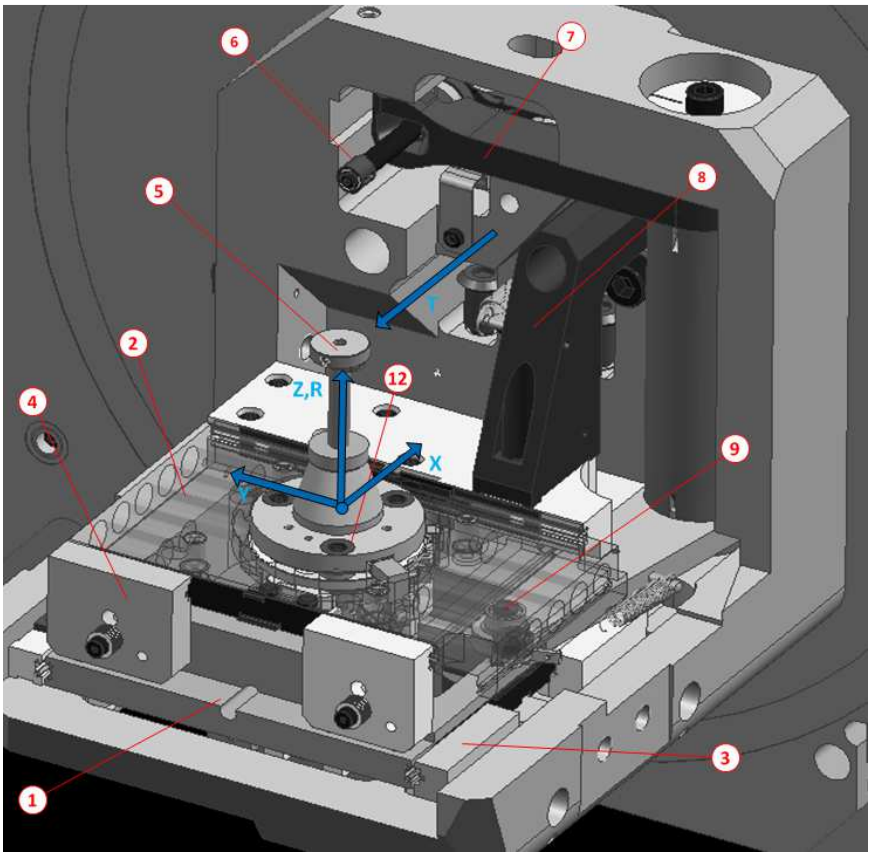

Picture 5 - stage mechanics

The Picture 6 is a top view to a 50mm DC stage. There is a RZ unit holding a sample which is carried in XY plane. Please note orientation of the coordinate system. The X linear guides ((3) in Picture 5) are mounted directly on the bridge and Y guides ((4) in Picture 5) are attached to X slide. In each axis one guide is always attached firmly and the other is pushed to its position by two independent sets of spring washers. This solution takes up the play even if the guides are not very precise. However, a serious disadvantage is that the guides have only two balls at each side which makes them insufficiently rigid (see 5 and 4.2.).

	stroke	**smallest step**	**max deviation**	**min speed**	**repeatability**
X	50 mm	0.5 mm	1%	5 mm/s	< 0.003 mm
Y	50 mm	0.5 mm	1%	5 mm/s	< 0.003 mm
Z	25 mm	0.001 mm	1%	5 mm/s	< 0.003 mm
R	unlimited	0.5°	0.030°	45°/s	< 0.1°
T	-15°… 75°	0.07°	0.025°	5°/s	< 0.1°

Table 1 - stage's parameters [4]

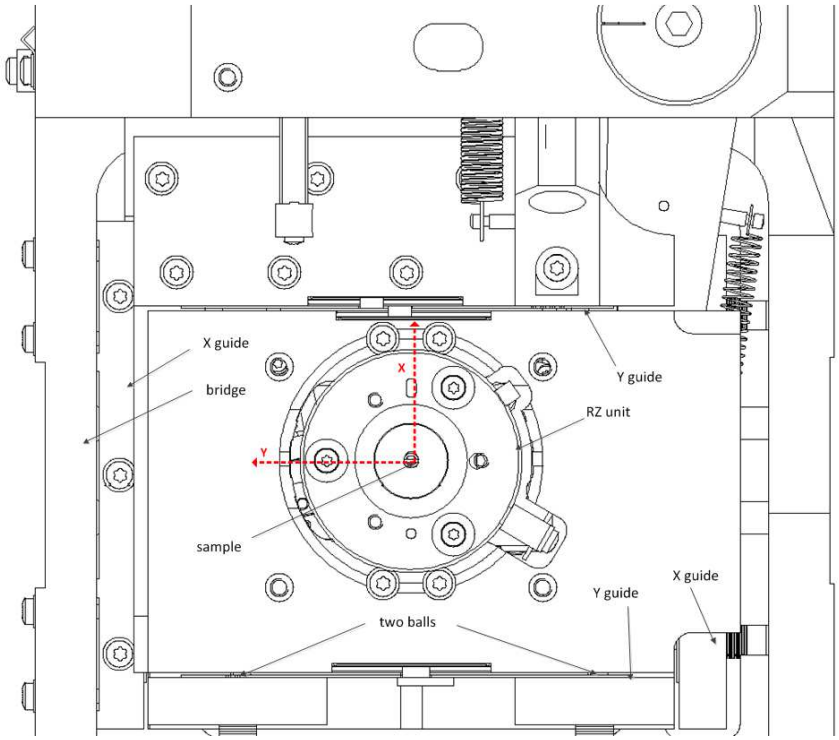

Picture 6 - top view of a stage

In Table 1 you can see a summary of a stage's parameters related to movement precision as specified in FEI documentation [4].

2.4. Repeatability

One of important parameters of every stage is so called movement repeatability. Although repeatability is not accuracy by the strict definition they are inevitably connected.

The Picture 7 illustrates the relation of accuracy and repeatability. A stage is supposed to move to certain *target position* and it makes an error. Then magnitude of this error is represented by accuracy. And when the same movement is performed repeatedly deviations in the magnitude are represented by repeatability.

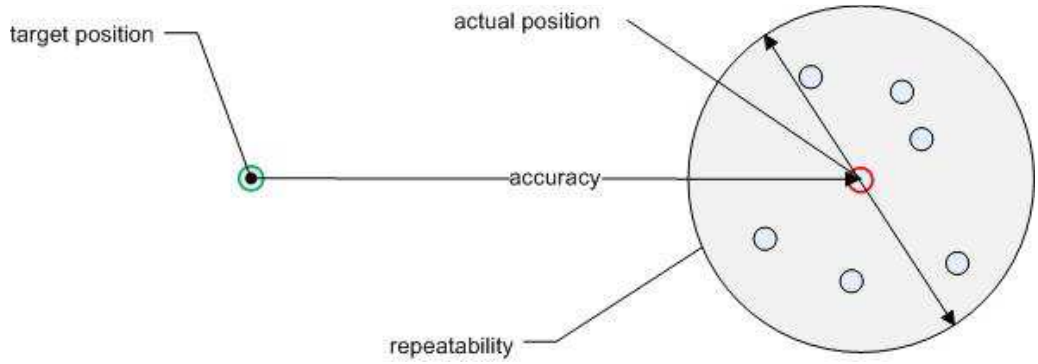

Picture 7 - accuracy and repeatability

That is why accuracy can be evaluated as mean value and repeatability as standard deviation of a set of movements.

However, it is impossible to make the very same movement twice in practice because the initial position cannot be reached precisely enough. And also while measuring motion on this scale, all moves are influenced by history of previous movement. This is caused by material hysteresis and solid friction among other things. Because of this repeatability is measured in a different manner.

When a stage makes two subsequent moves from point A to B and back along the same route it is possible to presume that on its way back to A it would reproduce all the errors it made on the way to B but in inverted order and with opposite sign. So a deviation which is measured at the end represents only random error and thus repeatability separated from the magnitude of accuracy.

FEI's low cost stages do not have specified maximum overall accuracy (some of the reason explained in 5.1.1) so repeatability is the main indicator of a stage's precision.

2.4.1. Measurement procedure

There is a prescribed procedure for repeatability measurement specified by FEI standards [5]. A stage makes series of movements in XY plane which are statistically evaluated afterwards. The mechanism which is being tested is tilted to horizontal position and centred in axes X and Y. The test itself starts with movement to relative coordinates [8mm, 8mm] and then back to the initial position. What is measured is difference in each axis between the initial and the final position. This end position of the first step is then considered as a start point for the second step and so on. The complete list of the movements is in the Table 2 and at Picture 2. Index *i* means that in each step a stage moves to the coordinates specified in the previous one.

i	Step 1 [mm]	Step 2[mm]
1	$[8_0,8_0]$	$[0_i,0_i]$
2	$[8_{i-1},5_{i-1}]$	$[0_i,0_i]$
3	$[8_{i-1},0_{i-1}]$	$[0_i,0_i]$
4	$[8_{i-1},-5_{i-1}]$	$[0_i,0_i]$
5	$[-8_{i-1},-8_{i-1}]$	$[0_i,0_i]$
6	$[-5_{i-1},-8_{i-1}]$	$[0_i,0_i]$
7	$[0_{i-1},-8_{i-1}]$	$[0_i,0_i]$
8	$[-5_{i-1},-8_{i-1}]$	$[0_i,0_i]$
9	$[-8_{i-1},-8_{i-1}]$	$[0_i,0_i]$
10	$[-8_{i-1},-5_{i-1}]$	$[0_i,0_i]$
11	$[-8_{i-1},0_{i-1}]$	$[0_i,0_i]$
12	$[-8_{i-1},5_{i-1}]$	$[0_i,0_i]$
13	$[-8_{i-1},8_{i-1}]$	$[0_i,0_i]$
14	$[-5_{i-1},8_{i-1}]$	$[0_i,0_i]$
15	$[0_{i-1},8_{i-1}]$	$[0_i,0_i]$
16	$[5_{i-1},8_{i-1}]$	$[0_i,0_i]$

Table 2 - repeatability movement [4]

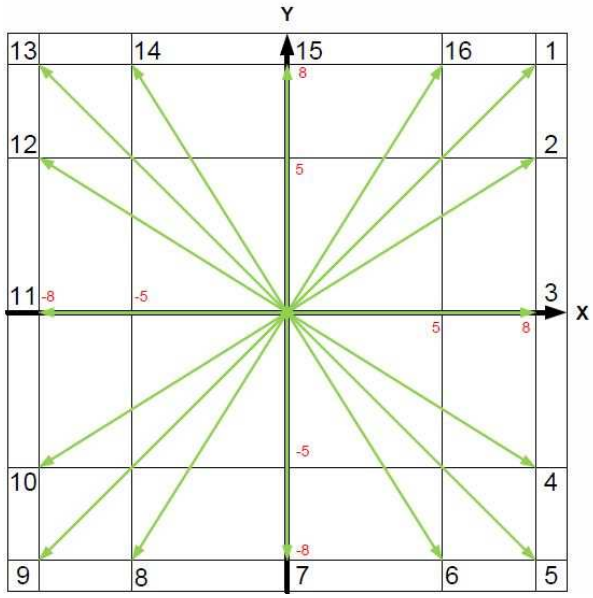

Picture 8 - repeatability movement [4]

The result of the test is then three times standard deviation σ of the 16 differences, which has to be less than 3µm (3σ<3µm). The reason why it is this way and not simply σ<1µm is that in normal distribution of error 3σ covers approximately 99.9% of values in the data set. Therefore it is guaranteed that the differences would be in span from -3µm to 3µm as the FEI specification defines. The method which is used for the measurement is explained in the 2.5.1.

2.5. Possible conceptions of repeatability measurement

2.5.1. Electron microscope

This is the way the measurement is actually done at FEI. The method is based on means of image processing. A sample with tiny (approx. 30µm - 50nm) tin balls is placed into a microscope (fixed to a stage) and then an image is acquired with magnification of 10 000x and resolution 1024x768 (Picture 9).

Width of the view is 30µm, divided by 1024 it gives 0.029µm per pixel which is theoretical resolution of the measurement. Subsequently a stage makes the first movement and another image is taken and is compared with the original one. And so on for the following steps. The procedure is performed with a microscope wherein the stage is permanently installed.

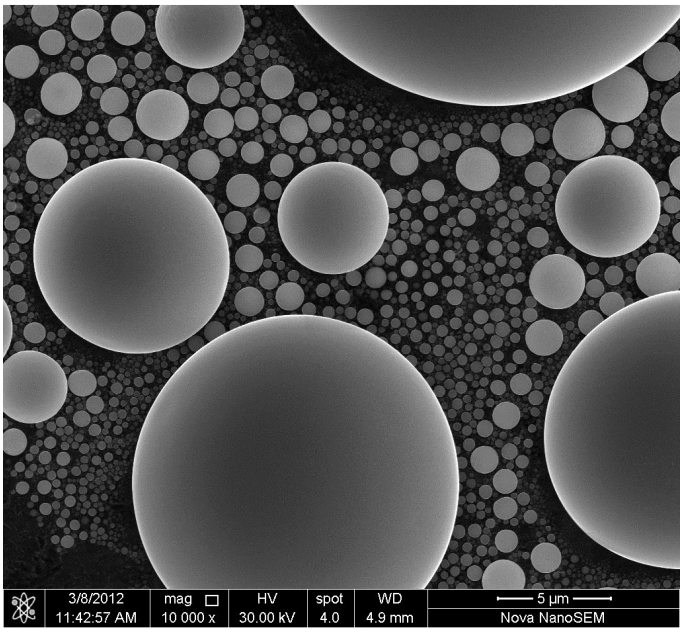

Picture 9 - tin balls

This is the most accurate method; resolution can be easily increased by higher magnification or image resolution. However, it has some disadvantages because of which it cannot be used at manufacturer's site. The first would be the price of the measuring device, even the cheapest electron microscope costs hundreds of thousands of dollars. The second problem would be maintenance and service as well as considerable environmental sensitivity of the apparatus.

Also measurement by an electron microscope is good for precise final validation of stage's parameters but it is not suitable for iterative adjusting process. It would mean pumping out the chamber and setting up image after each slight adjustment which would be very time consuming. And it is also redundant to use such a device only to measure two displacements. It is obvious that finding different solution is the main task of this work.

2.5.2. Optical microscope

An optical microscope using the same methods would seem to be a reasonable alternative but there are some reasons why it cannot be done. It has been shown above that maximal resolution of classical microscope is slightly less than 200nm. The range of the measured deviations is in range of units of microns so it still could be used somehow. The problem is that these results can be obtained only under perfect circumstances and only with high-end, which means expensive, microscope so it almost leads back to an electron microscope. There are also X-ray microscopes available, they

have higher resolution than those using visible light but they suffer from all the disadvantages mentioned too.

2.5.3. Specialized displacement sensors

The two previous considered solutions were based on using very sophisticated apparatus in the way they weren't originally intended to be used. Nonetheless there are many specialized displacement sensor which are more suitable for the task.

From the wide range of displacement sensors there are five principles with which required (submicron) accuracy can be achieved: inductive, eddy currents and capacitive sensors, triangular laser and precise encoders.

Along with demand for accuracy there is another one for measuring range or at least measuring distance. Meaning that it would be preferable to measure movement in the whole range of 16 mm and if it is not possible a sensor should be able to operate from sufficient distance to not obstruct the movement which would be at least 8 mm. This second requirement leaves out capacitive and eddy current sensors. Those with sufficient accuracy have too short operating range (for example [6]).

The both requirements mentioned in the previous paragraph could be met by a proper linear inductive sensor. However, this kind of sensors has to be physically attached to a base and a moving element. This is not problem for a permanent installation but in the case of repeatedly mounted and dismantled device there are concerns about damaging the sensor by human fault. That is why this solution has been rejected.

A triangular laser sensor could satisfy all the demands and one also has been purchased in early phase of this project. However, it has proven to be too complicated to design proper mounting because the transducer itself is relatively big and heavy (see 3.1) and there were serious issues with vibration. Nonetheless the laser has been implemented as additional sensor to measure Y linear guide play (see 3.2).

So there is only one option left from the list above which is an encoder. At first sight it may seem odd to use encoders for measuring behaviour of a device controlled by encoders as well but it must be noted that these would be of completely different accuracy class and be placed directly at the stage, not at the end of the gear chain. Thus encoders RGH24Y made by Renishaw were used from the wide spread of displacement sensors (see 3.1).

3. Measurement tool

The purpose of the test tool designed here is to provide a sufficient measuring device to a third party manufacturer of the stages so they could validate parameters of a stage before delivering it to FEI. The mechanisms have been assembled by a couple of skilled and experienced workers for many years without precise gauging and there were not many problems. However, due to recent rise of production new assemblers were hired and time have become more important asset which has brought need for some kind of accurate repeatability test tool.

The device itself consists of four distinctive parts – sensors, mechanical parts, hardware and software. They are thoroughly described in this chapter.

3.1. Sensors

Two kinds of sensor have been used, previously mentioned linear encoders Renishaw RGH24Y and a triangular laser displacement sensor Micro-Epsilon ILD 1700-2 which operates in combination with one of the encoders.

3.1.1. Encoders

The encoders which have been used are linear Renishaw RGH24Y with resolution of 0.1µm [7] . These had been purchased and installed on improvised measurement device which preceded the one described here. Because the step of the encoders is smaller than the wavelength of the laser used [8], the encoders utilize so called integral interpolation [7]. Encoders based on this principle use interference when a light pattern generated by encoder's scale and a mask in front of a photo-detectors provide two sinusoidal signals with phase shift of 90°, instead of simple pulses like a quadrature encoder [9]. Picture 10 shows the principle of generation of an interference pattern in an encoder made by Heidenhain company, it is common to all the interpolative encoders. In the picture, C is grating period of the reticle and the scale, Ψ is phase shift of light wave when passing the scanning reticle and Ω is phase shift caused by movement of the scale.

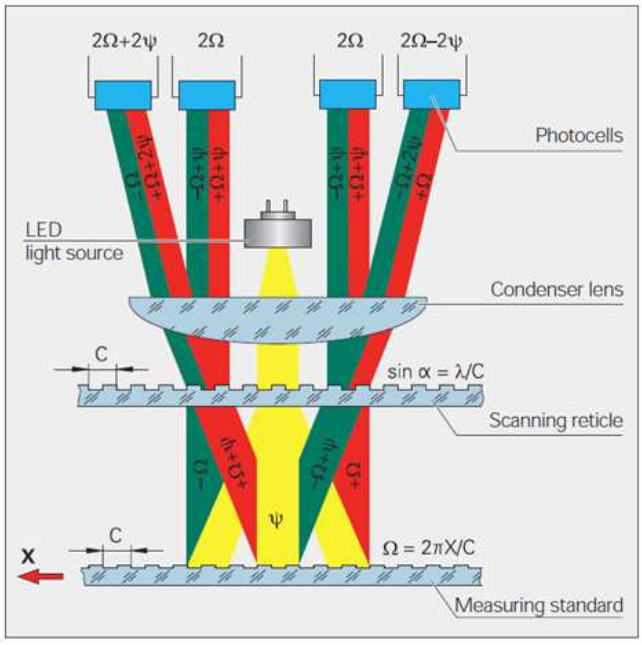

Picture 10 - Interferential scanning principle – Heidenhain [10]

These signals are afterwards processed by sets of differential amplifiers which generate pulses. Based on signal's quality, this quantization can provide higher resolution than the encoder's scale pitch is. Simple zero-crossing detection gives 4-times scale's resolution [9]. For example RGS20-S scale for RGH20 series has pitch 20µm [11] which corresponds with 50 quantization levels for readhead RGH20Y. The encoders provide standard TTL quadrature output. Also a great advantage of this type of encoder is their robustness and that the scale can be stuck to wide range of surfaces. The sensors are equipped with a signal LED that shows quality of alignment.

Picture 11 - RGH24 series readhead [7]

3.1.2. Laser distance sensor

This sensor is used to measure the play of the Y linear guide. It has been purchased for evaluation purposes for FEI's product engineering department at the beginning of the project. At first it was supposed to be used as the main

displacement sensor but it has turned out that proper attachment would be unreasonably complicated.

Micro-Epsilon ILD1700-2 is a laser triangular sensor. Its principle is simple. *"Triangulation means the measurement of distance by calculating the angle. In measurement technology a sensor projects a laser spot onto the measurement object. The reflected light falls incident onto a receiving element at a certain angle depending on the distance. The distance to the measurement object is calculated in the sensor by the position of the light spot on the receiver element and from the distance of the transmitter to the receiving element* [12]." The receiving element is a CCD chip with high resolution.

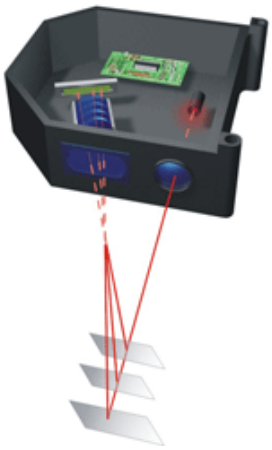

Picture 12 - laser triangulation [13]

This particular laser has resolution 0.1µm and measurement range of 2mm (from 24mm to 26mm). Its sample rate can be up to 2.5kHz, however, according to recommendations in the manual it has been set to the lowest frequency possible, 324,4Hz [14]. It is so because the sensor cannot handle full speed measurement if the target object is slick. The aluminium reflective surface used as a counterpart has relative roughness 0.8 which makes it shiny.

The roughness 0.8 might still seem to be too much considering the resolution of the sensor but the laser spot has diameter 80µm so separate inequalities do not inflict the results. The transducer also provides inner sample buffer and it is to set to return a mean of 128 samples to filter eventual noise.

3.2. Mechanical part

The only purpose of the mechanical parts of the tool is to provide proper and stable attachment for the sensors and their complementary parts. The requirements for these components were to be easy to mount on and to dismantle off a stage, to be easily adjustable and what is the most important it had to be done without modifying the stage itself. It would be simple to add several high precision holes and fix everything to them but there was a condition of backward compatibility. It was necessary that tool could be used for all the stages including those which are ten years old and came back from the field to be repaired. So all the mechanical parts were designed with relatively loose dimensions, on the other hand it makes them easily adjustable. The Picture 13 shows the assembly of the mechanical parts and the sensors. The denoted dimensions are working distances of the transducers and are based on datasheets [14] and [7]. Particular mechanical components are described later on and Table 3 is bill of material of the device.

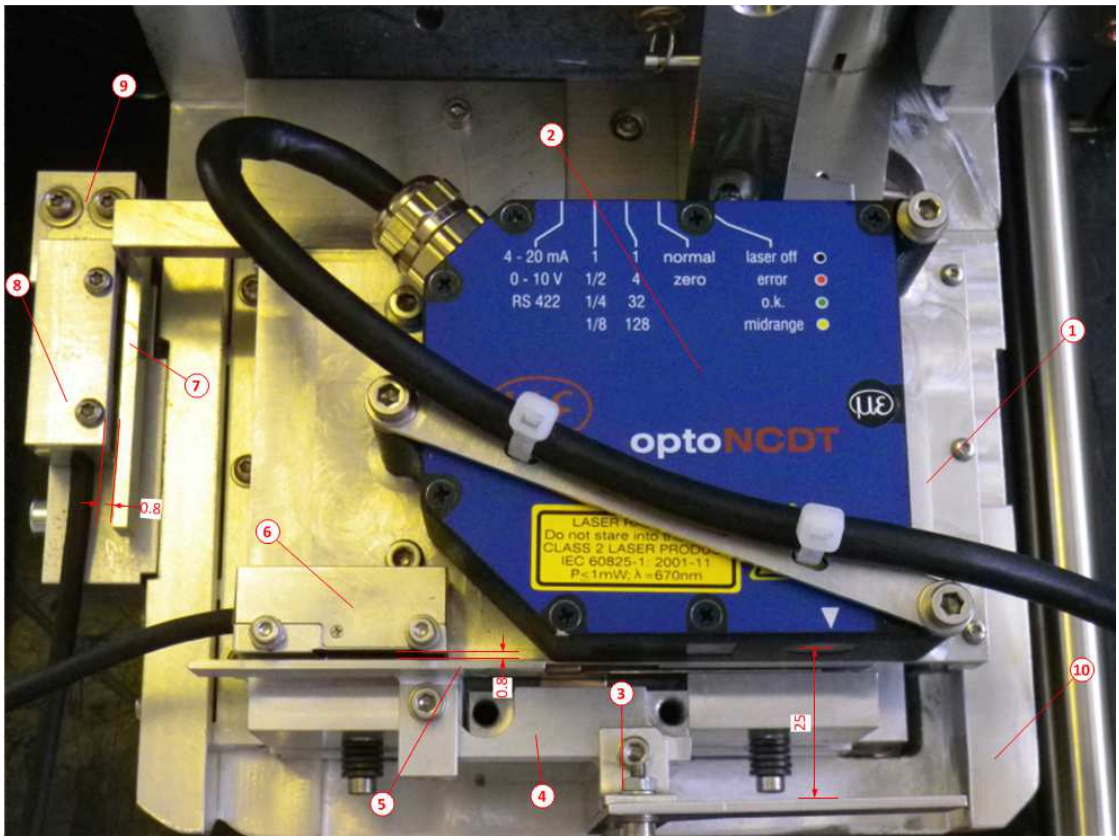

Picture 13 - measurement device

ref.n.	part
1	laser and Y encoder holder
2	triangular laser sensor
3	reflective surface
4	Y encoder and reflective surface assembly
5	Y encoder scale
6	Y encoder
7	X encoder scale
8	X encoder
9	X encoder holder assembly
10	bridge

Table 3- measurement device BOM

Laser and Y encoder holder (1) is a plate which carries the laser sensor and the Y encoder. It is aligned to the Y slide (Picture 5) and fixed to the position using threaded holes on the left side. These holes are for attaching custom stage equipment under normal circumstances.

There were certain concerns whether the sensors can be placed in this manner because it means that stage carries them all the time. The laser itself weights over 500g [13] and with the platform total mass reaches almost 700g which is many times more than a usual sample. However, a stage has to satisfy the specifications which say that it has to be able to carry weight up to 1000g [4] when not tilted with accuracy within limits (in Table 1). And some off standard FEI's equipment weights approximately equally so this can be even considered a load test of a kind.

Y encoder scale and reflective surface assembly (4) is a complementary assembly to the laser and Y encoder holder. It consists of a reflective surface for the laser measurement of the Y guide's play, a facet where a Y scale is stuck and a block which is attached to a stage. Both the scale and the reflective surface are longer than it is necessary. Originally it was intended to analyse stage's movement in its whole range but the available (3.3) hardware did not allow that.

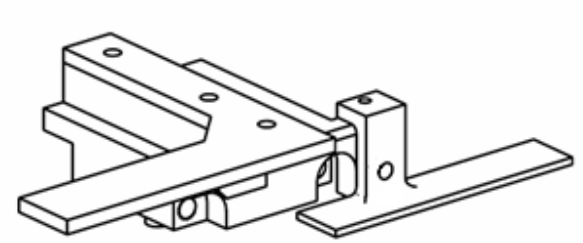

Picture 14 - Y scale and reflective surface assembly

The assembly is attached to the X slide using one of production holes. A pin is inserted in the hole and it is fixed by a couple of headless screws. Assembly's main block is aligned to a vertical plane on the stages X slide so it is parallel to the encoder's readhead and perpendicular to the laser beam. Because an error in stage's movement is even smaller than diameter of the laser dot this aligning is sufficient for the reflective surface. But the encoder scale has to be parallel with deviation smaller than 0.1mm [7] at 16mm range and because of that it can be set independently.

The X axis measuring encoder is carried by X encoder holder assembly (9) which is mounted on the side of the stage's main bridge using two production threaded holes. It consists of two parts; the encoder is firmly fitted to the one which can be adjusted with respect to the stage.

X encoder scale is stuck to the last designed mechanical part (7). The component is carried by the stage's X slide and is aligned in direction of axis X.

3.3. Hardware

Picture 15 shows how the used hardware is connected together. Components in the cornered rectangles are standard parts used in a control chain of Quanta microscope. Those in round rectangles are external sensors described above. High level control (user interface) is handled by a microscope PC (MPC) which communicates with NYCE4000 motion controller. It feeds stage's motors with DC voltage and reads feedback encoders. The additional sensors communicate with the MPC via RS232 interface (the laser uses RS422-RS232 converter). Detailed description of individual components follows bellow.

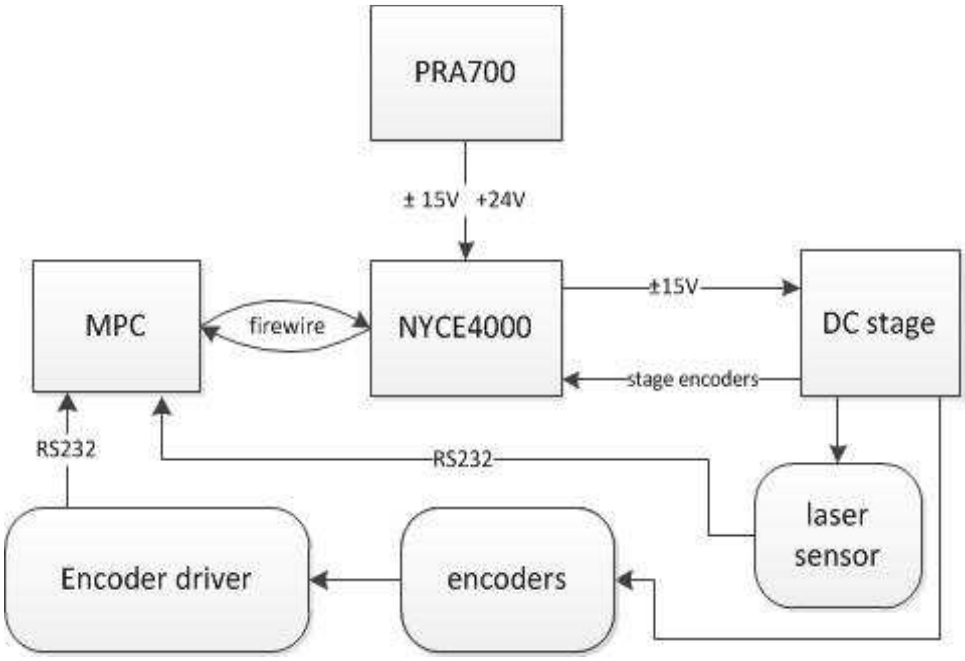

Picture 15 - hardware schematic

A MPC is a standard PC equipped with a firewire card. It runs Windows XP, server application and a test-tool's user interface (see details 3.4). It serves as a host computer for NYCE4000.

PRA700 is a power source made by PBF group. It provides power for NYCE4000 motion driver and DC motors.

The great majority of FEI's stages are controlled by NYCE4000. It is a modular motion controller made by Bosch Rexroth. Each system contains a motion control unit (MCU) and a number of drive modules in a common housing [15]. The MCU used in this case is NY4110. It communicates with a MPC via firewire, can run up to ten control loops of a motor and handles power electronics [15]. Stages can be either speed or position controlled. Both modes use PID controller with feed-forward (see 3.4.1). The other modules are NY4130 - DC drivers, they embody power electronics and (feedback) encoder reading. These are not PWM drivers so stage's motors are driven directly by DC voltage. Each NY4130 can handle two servos [15] so for the case of 50mm DC stage with manual tilt there are two of them. This configuration of the test device can be used for a stage with motorised tilt as well because T axis is not related to repeatability measurement. The last module is DCMAB which controls low-level safety functions and switches off movement if necessary.

Picture 16 - NYCE4000

The encoder driver was manufactured by a Czech firm ESSA and is based on ATMega16 chip. It has three encoder counters but only two of them are exercised however. It is relic of the improvised test used previously. It has been implemented to the test tool in attempt to save money. It is too slow for sending every tick (maximum frequency is approximately 300Hz [16]) and it has proven to be unreliable during the project so original National Instruments PCIe-6230 data acquisition card has been purchased as a replacement but not yet implemented. But a software solution using this driver had been made before that and it is described below.

3.4. Software

Once the sensors were chosen and the mechanical part was ready, it was possible to start developing software. The assignment of the thesis was to create user interface which would allow performing whole repeatability measurement from one screen including homing a stage and user defined stage movement.

This interface has been programmed in Labview environment for various reasons. Generally, Labview is specialized in measurement applications. It allows creating lucid and user friendly Windows programs very easily and has native support of wide range of specialised hardware made by the same company, National Instruments. Although no such hardware was available at the beginning of the project, it provided possibility of further improvements. And all the Micro Epsilon's laser distance meters are provider with a complex suite of Labview VIs that interface serial ports via special dll.

So the issues to be solved at this point were: settle communication between MPC and additional sensors, resolve connectivity to NYCE4000 (XTlib.dll see 3.4.1), collect measured data and evaluate them, archive data and create stable and fool-proof user interface.

3.4.1. Software motion control

All the FEI microscopes have the same structure of their software control. In the Picture 17 is a schematic of it. Typically there are two computers connected via ethernet. A Support PC (SPC) is optional and it is not directly connected to a microscope, it can run support or office programs and be connected to other networks.

The computer that really controls a microscope is MPC. It is a Windows based PC (XP or Seven) and Microscope Server [17] instance runs on it. This application controls the whole microscope, electron and ion emission, lenses, detectors, a vacuum pump and, what is important for this thesis, a stage. Normally all the functions are controlled via FEI XT User Interface or by a bundle of FEI service tools but there is a dynamic library which serves as a program interface for a third party programmers and which has been used for designing the test-tool's interface.

Every stage can move in three modes based on the way it is controlled. First one is movement in open loop when voltage is directly applied to a motor without feedback. This mode is used only for some special diagnostic procedures. The second is so called *jog*. In this case a stage runs in speed control mode when speed information is differentiated from position.

The last mode is *point-to-point* motion. Here the desired value represents position. However, PID for position control is slow with great integrate constant to be as precise as possible so a stage starts motion in speed control mode and when it is close to the desired position, controller is switched to position control. There is one more feature implemented to improve precision of the movement. When a desired position lies is direction that shrinks the spring which prestresses the threaded rod (see 2.3), the stage purposely passes its destination and then returns to the desired position. This way it always approaches the position from the same direction which winds up the spring and thus eliminates play.

3.4.2. XTLib

XTLib is an interface dynamic link library (DLL) provided by FEI to third party software developers and provides full control of a microscope and its peripherals. The Picture 17 shows a block diagram of interfacing server application via this library.

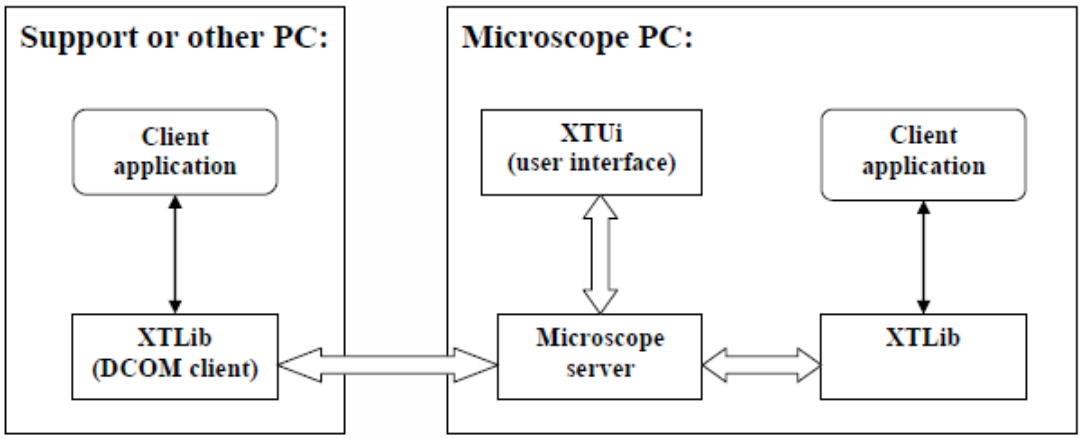

Picture 17 – XTlib [17]

"XTLib consists of a series of COM objects that forms a naming and containment tree convention. This partitioning of functionality and control into objects allows users to locate and operate on an object that encapsulates and abstracts only. Parent and child objects form this containment tree where parent objects can contain one or more child objects. Child objects themselves may be parents to one or more child objects as well [17]*."* The tree structure approximately represents physical functionality of an electron microscope. The whole library is too complex to be presented here as a whole but objects that have been used in the program are thoroughly described below.

3.4.3. Client application

3.4.3.1. Accessing shared libraries in Labview

Two separate shared libraries have been used in this project: MEDAQlib.dll for communication with ILD1700-2 laser and XTLib.dll to control a stage.

MEDAQlib library is provided by Micro-Epsilon company. Although full documentation of a communication protocol is available, using MEDAQlib allows programming at higher level and makes the program more lucid. Micro Epsilon even grants sample VIs, however, they are simply wrapped standard Labview "call library" functions. All input parameters and settings used in the client application have been taken from Micro-Epsilon industrial manual – Data Acquisition Library [18].

The Picture 18 shows an example of opening a new laser instance using prefabricated VIs. It is very illustrative – demonstrates choice of a sensor type, setting serial link and open the instance.

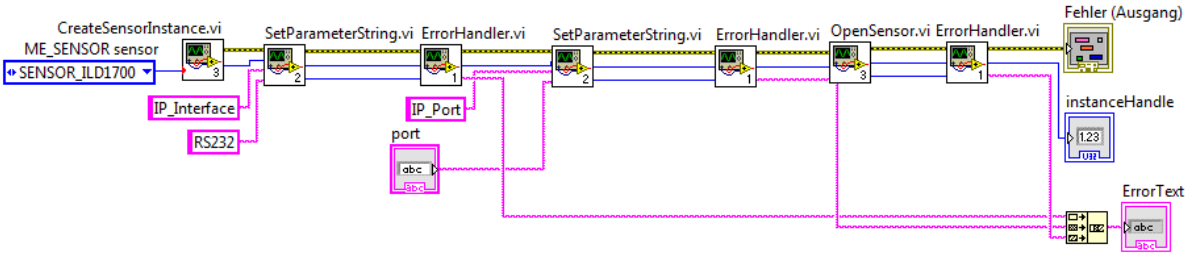

Picture 18 - opening laser instance

What is actually hidden inside the VI shows Picture 19, each VI contains simply "call library function" which can be used to call any win32 library. This block requires a path to the dll, then it is possible to choose a function to be used and to define function prototype in a C like format. All the communication with the laser is handled in this manner.

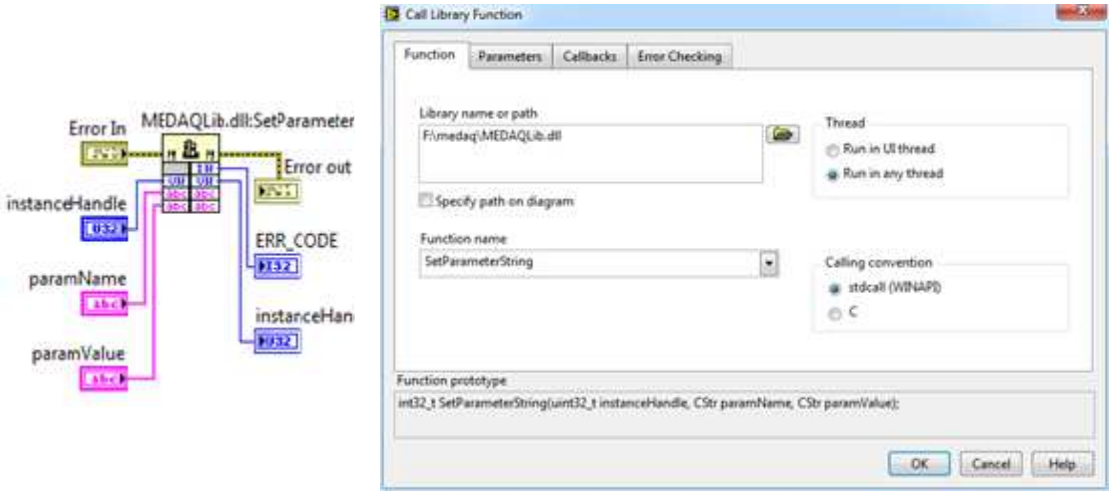

Picture 19 - calling a dll

Unlike MEDAQlib, XTLib is a .NET assembly using COM specification [17] as such, it has different inner structure although they both have .dll suffix [19]. So it must be accessed in another way using constructor nodes for creating an instance of XTLib and then a sequence of invoke nodes to access desired object [20]. For example function "MoveDelta" is for moving stage relatively, it is in object MicroscopeControll.StageControl [17]. In the Picture 20 is an example of calling this function. There is also function "Connect" called because:*"This function has to be*

called after creating MicroscopeControl object to be able to access all other functionality of XTLib. This method internally sets connection between XTLib and local or remote instrument depending on parameter strMachineName. [17].”

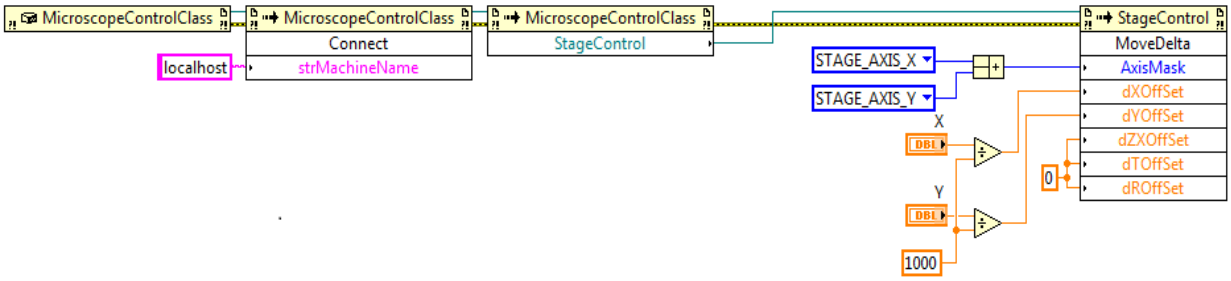

Picture 20 - XTLib example

The example schematic moves stage relatively in axes X and Y (according to the mask) by the distance specified by controls X and Y. This structure is used in the client application with a small exception of homing separated axes for reasons explained in 3.4.3.

3.4.3.2. User interface

The user interface has been designed to be simple and follows the simple rule that a user should not be bothered by unnecessary information and should not get chance to break anything. The whole measurement process is controlled by the five large buttons on the right side. They represent steps which have to be done during the test and each of them stays disabled until the previous step has been completed successfully. So at first a user sets up all the mechanical parts and connects stage and sensors to a MPC. Then he has to home axes X and Y because the feedback encoders are incremental. After that it is possible to test whether the sensors are connected to the right USB ports and if the measurement encoders are aligned properly. And after that a user is allowed to start a repeatability test. The last two buttons are to stop the test prematurely and quit the program.

The only thing a user has to fill in is a serial number of the stage being tested. Information displayed during measurement is: number of a current movement, deviations and current 3σ for each axis and whether a stage is passing or not so far (red or green indicator).

There are two buttons which are not directly related to the testing but might be very useful they allow a change of an archive file and point to point motion in XY.

The user can also see what action the program is performing at a time (initialization, homing etc.), these states are thoroughly described below.

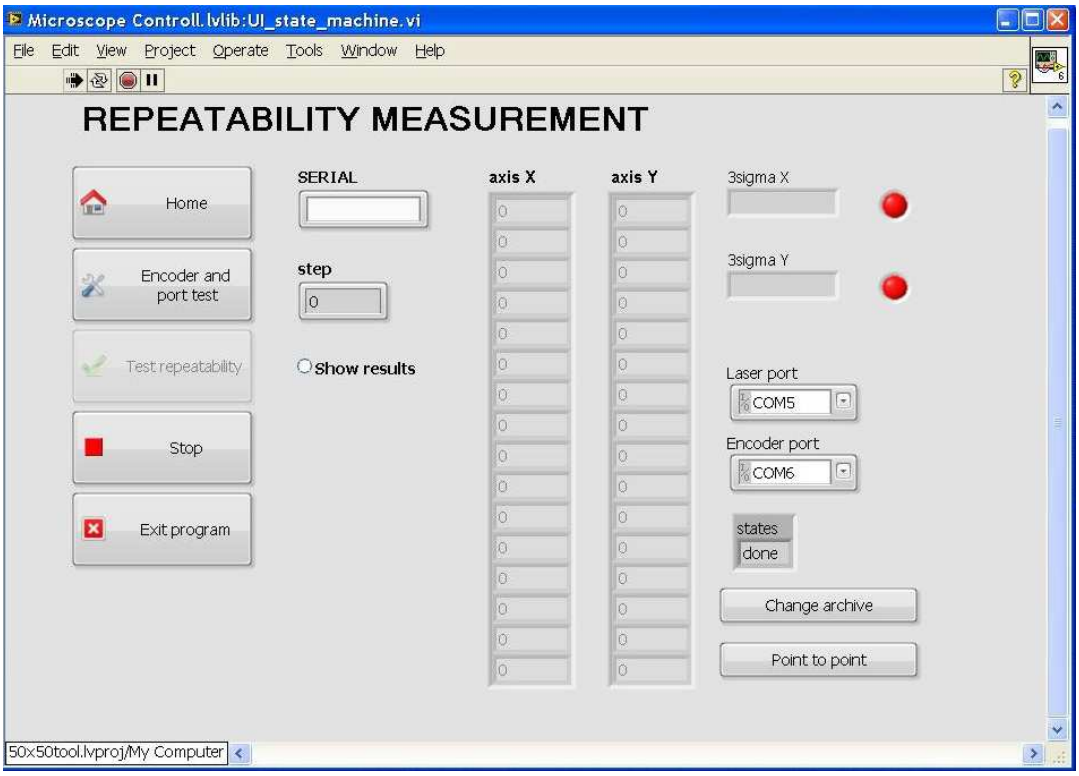

Picture 21 - user interface

3.4.3.3. Client application as a state machine

When the client is started the first thing it does is initialization of variables from the front panel, disables buttons and finds the archive file.

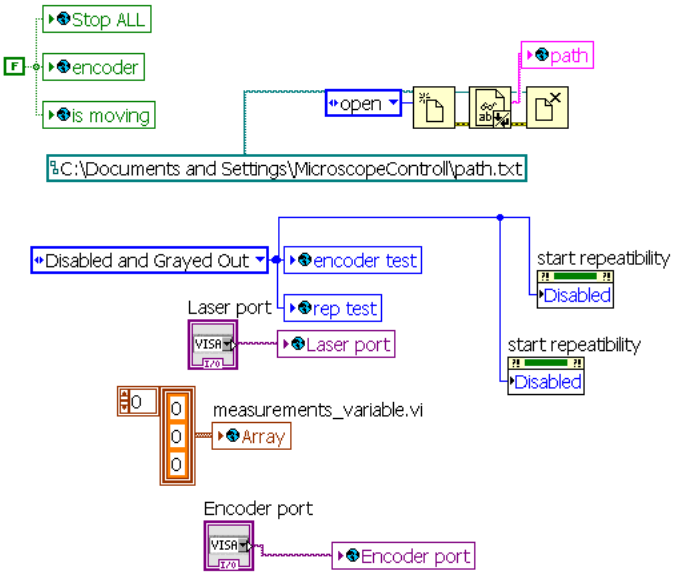

Picture 22 - initialization of variables

Three loops which run until the end of the program are initialized in the following step. They are shown in the Picture 23. The loop in the left updates the user interface twice a second with measurement data and status of the buttons.

The loops on the right are more interesting because they represent the state machine itself. They work with a queue of states which was initialized by the two green VIs to the left (and XTlib instance is created there). The bottom loop waits for events in form of value change in the front panel (a button is switched). When an event occurs it adds specific item to the end of the queue. The second loop is runs ten times a second and the state handler VI inside dequeues item by item and initializes a state with respect to it.

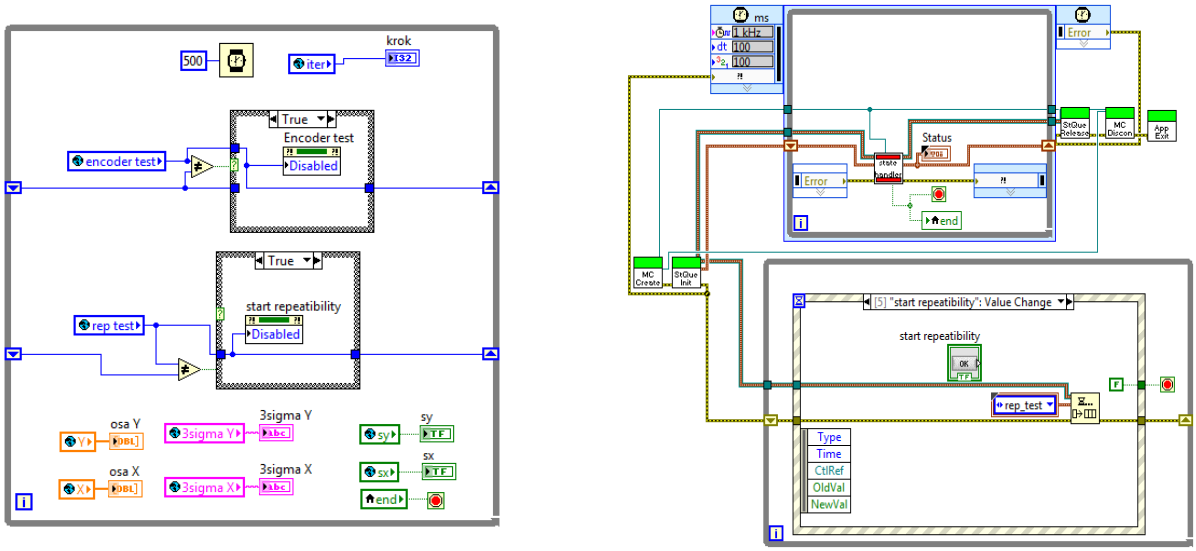

Picture 23 - user interface schematic

This structure allows handling situation when a user clicks on multiple buttons before current operation is finished because every action on the front panel is added to the queue. It also saves computer time, when there is no action demanded by a user the only things that are running are slow UI update and almost empty loop waiting for an event.

3.4.3.4. State handler

In the Picture 24 is a partial schematic of the state handler VI mentioned in the previous section. Like in every Labview code a data flow left to right so it takes the oldest item from the queue, checks the queue for errors and then chooses what action to take according to the item (there is a special case for choice a user can make). The following paragraphs describe individual states that can occur.

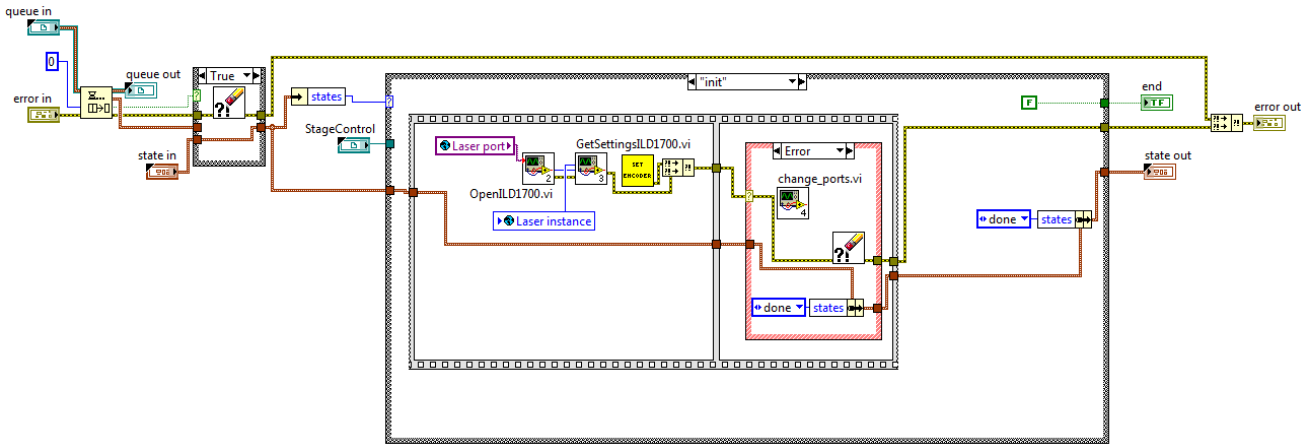

Picture 24 - state handler

Initialization – *init*

This state can be seen in the Picture 24. It initializes COM port for the encoders, create laser instance and verifies whether they are connected. If not, it opens a dialog to change the ports.

Homing stage – *home*

Homing is a procedure which serves to determine absolute position of a stage. All FEI stages use relative encoders so it is necessary to find zero position and thus set up a coordinate system somehow else. In the case of X and Y axes a stage starts to move towards a hard-end stops slowly in speed-control mode. When it hits the stop an instant drop of speed is detected and the coordinate of the axis is set to its lower limit (-25mm). Some other stages use limit switches or index point on a scale but the idea of homing stays the same.

The function for homing axes separately can be found in a different object than "MicroscopeControll.StageControl", it is in the part of XTLib library that was added later and is called "MicroscopeControll3.StageControl3" which has its own interface [17].

The following piece of C# code was compiled into a .dll to create instance of MicroscopeControlClass and retypes pointer from IMicroscopeControl to IMicroscopeControl3 and thus accessing this pointer and MicroscopeControl3 object and its functions. It also accesses StageControl3.HomeAxis object to home axes X and Y. There is no need to home other axes for they are not used during the test.

```
namespace HomeClass
{
   public class Home
   {
      public static void Load(XTLIBLib.StageAxisMask mask)
      {
         //empty pointers
         XTLIBLib.IMicroscopeControl m_microscopeControl = null;
         XTLIBLib.IMicroscopeControl3 pIMicroscopeControl3 = null;
          //constructor for IMicroscopeControl
         m_microscopeControl = (XTLIBLib.IMicroscopeControl)new XTLIBLib.MicroscopeControlClass();
         //queryinterface, poiter to changed type  IMicroscopeControl to IMicroscopeControl3
         pIMicroscopeControl3 = (XTLIBLib.IMicroscopeControl3)m_microscopeControl;
          //connect microscope
         m_microscopeControl.Connect("localhost");
         //load stagecontrol
         XTLIBLib.StageControl3 stageControl3 = pIMicroscopeControl3.StageControl3();
         //call HomeAxis
         stageControl3.HomeAxis(mask, true);
      }
   }
}
```

After homing a stage, VI enables Encoder and Ports Test button.

Encoder and port test – *enctest*

This state checks if the sensors are connected and moves a stage in the whole range needed for the repeatability test. If everything is alright it enables Repeatability Test button. The encoder test can detect whether the sensors are connected and are at correct COM port. If the is a problem, the dialog stays opened and the user has to either change software port or resolve hardware problems and run the test again.

Repeatability test – *reptest*

This is the most important state because it is where the measurement is executed. It is a sequence of VIs.

First of them searches the archive TDMS file for the serial number entered by a user and the highest number of measurement assigned to the serial. If it finds nothing, sets number of measurement to 1. Otherwise it increments the highest number by 1. TDMS is specific National Instruments' structured file format.

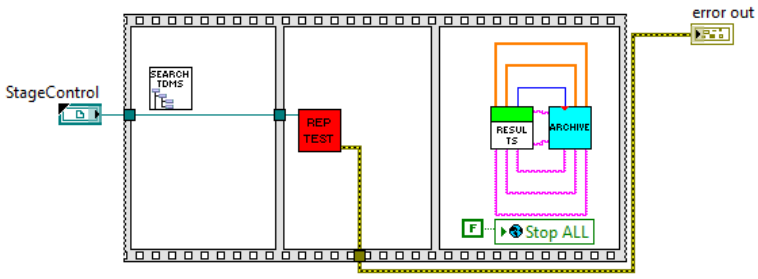

Picture 25 - repeatability state schematic

The next step of the sequence is the repeatability test itself. The red VI Rep Test (Picture 25) contains two parallel loops. The first is simply for reading the external encoders, after resetting then by ASCII string [16] (Picture 26). It sends a request for position at 100Hz in ASCII, receives reply string, extracts position data from it and writes it into variable "actualposition". This solution might seem senseless for two reasons. First, why to check position all the time when it is needed only at the end of each movement? Second, if reading continuously why so slow as 100Hz? The answers come from experience with unstable behaviour of the encoder driver. This low cost piece of hardware manifested unpredictable behaviour when a reading request was sent in bigger time gaps. Meaning that when position was read only when needed (once in 2 seconds) the driver send wrong or incomplete data and ended in error eventually. It was found out empirically that increasing frequency of the reading request supressed this problem. It might indicate issue with timing or with counters' buffers but without thorough insight to the hardware and firmware of the driver it is difficult to resolve. And 100Hz is sufficient frequency to both avoid the data problem and still provide information needed because a stage stands still for 100ms after each movement.

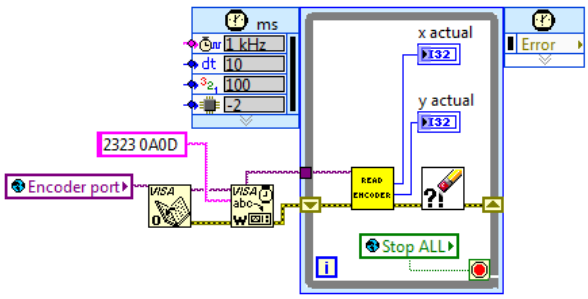

Picture 26 - encoder reading

The second part of the measurement VI is in Picture 27, it works in two phases. In the first it moves a stage to the position [0,0], waits for 1000ms and then reads the encoders and the laser sensor. The obtained information is written to a cluster

(Labview structured data type) and is considered to be initial position for the measurement. In each iteration of the following loop a stage makes a movement required by the prescribed procedure, sensors are read and the cluster containing all the measurements so far is sent to a statistic VI. The dwell times between movements and before measurement are meant to allow the stage to stabilize itself.

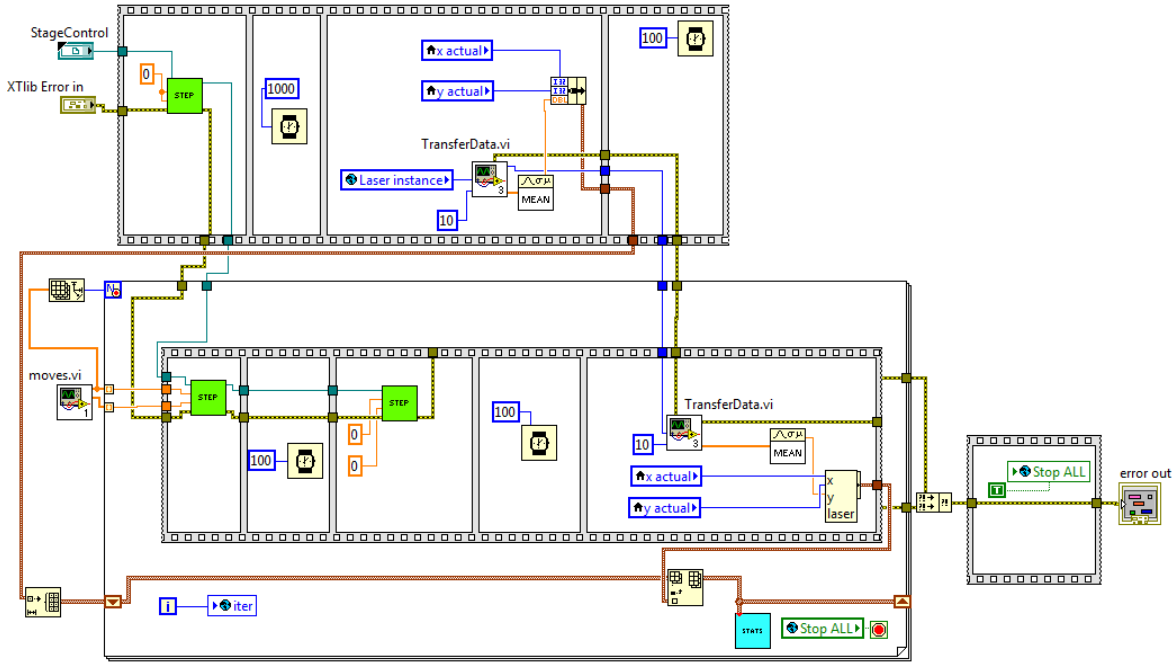

Picture 27 - repeatability VI

The statistic VI processes data according to equations (2)-(4), where $\tilde{x}_i$ is overall deviation in axis X, x_i is position given by X encoder and $\bar{x}_i$ is distance given by the laser.

$$\tilde{x}_i = (x_i - x_{i-1}) + (\bar{x}_i - \bar{x}_{i-1}) \tag{2}$$

$$\mu = \frac{1}{n}\sum_{i=1}^{n} \tilde{x}_i \tag{3}$$

$$\sigma = \sqrt{\frac{1}{n}\sum_{i=1}^{n} (\tilde{x}_i - \mu)^2} \tag{4}$$

The calculation is done the same way for Y, except there is only encoder data. The VI checks if 3σ < 3μm and sends all the results to the user interface in each iteration.

The measurement can be interrupted by the Stop button on UI.

Once the measurement is done all the data are archived into a TDMS file. The file has following lucid structure:

- serialnumber1-number of measurement1
  - deviations X
  - passed in X
  - deviations Y
  - passed in Y
- serialnumber1-number of measurement2
  - deviations X…

The file contains data of every measurement ever done with the test tool so it would be possible to compare result of a stage returned from the field and so on. Number of the archived results is limited only by the file size that NTFS system can handle. a user can choose whether to open the archive at the end of the test to see older entries. TDMS files can be easily converted to .xml or .xls files.

This repeatability state ends with writing *false* to StopAll variable so it can be run again.

Point-to-point – *ptp*

This is an additional VI which pop-ups a simple dialog to move a stage in XY. OK Button calls “MoveDelta” function and then reads stage’s position with “GetPosition”. Cancel button closes the VI.

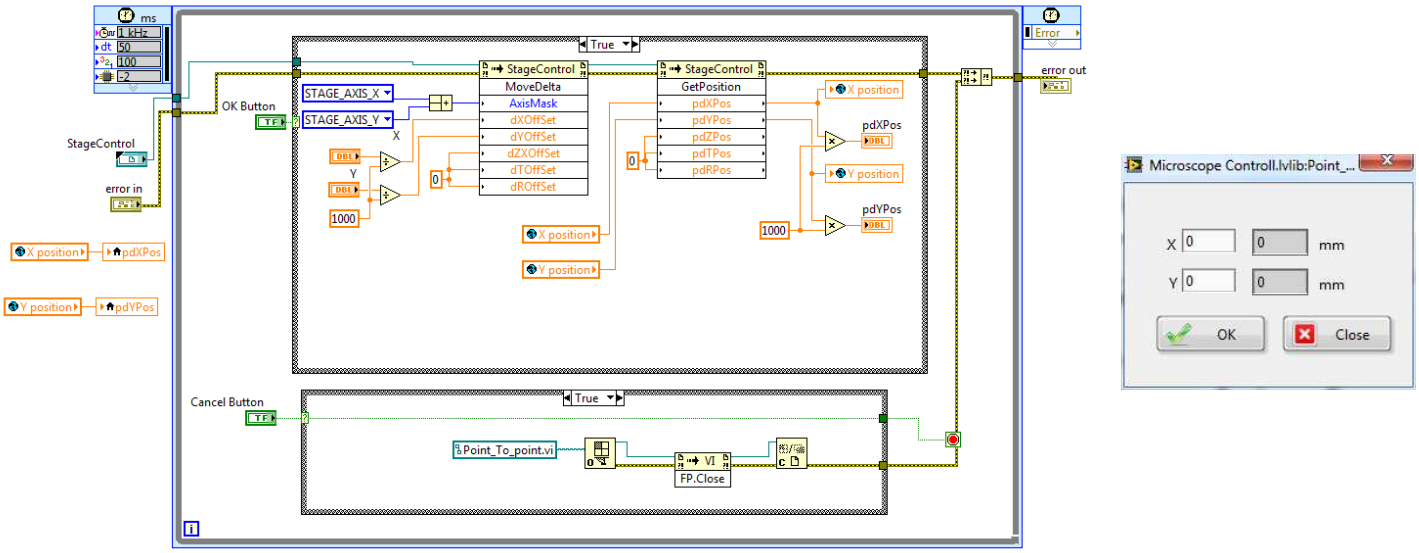

Picture 28 - Point To Point

Change archive – *change file*

The VI with very similar front plane to Point-to-point, allows changing file to archive acquired data. It changes a way to the archive in variable “path” and stores the path to a text file for the next start-up of the program.

4. Stage redesign

4.1. Stage issues

From the point of view of FEI, problems with the 50mm DC stages can be divided into two categories. The first could be called “there is still room for improvement” and covers issues may cause troubles to FEI technicians while adjusting or repairing a stage. Although these do not have any influence to functionality at all.

Problems that cause that a stage does not satisfy specifications or does not work properly are in the second category, such issues are gathered in FEI’s quality database. There have been **246** of these considering 50mm DC stages in 2010 and 2011 together.

issue	count
vacuum leak	8
repeatability	138
drift	10
electronics	12
other mechanical	37
Z - fall	26
other	15

Table 4 - stage issues

repeatability X	118
repeatability Y	76

Table 5 - repeatability number

Particular problems summarized in Table 4 are explained in following paragraphs.

Vacuum leak

Because a stage is placed in a vacuum chamber it is necessary that it is vacuum-tight. To seal all moving parts (shafts) entering the chamber is rather difficult task because the order of vacuum required is up to 10^{-5}Pa. However, all the problems that occurred were to a human error during assembly and there is not any reason to interfere with the design.

Z–fall

When Z axis is set to the eucentric height an image should stay focused during tilting of the stage (see 2.2). Play in tilt bearing and its fit causes that whole stage drops in vertical direction by hundreds of micrometres which manifests by defocusing of the image. There is no way to automatically detect and correct this event because the only

sensors detecting position of a stage are encoders outside a chamber. New flange has been designed as well as new bearing chosen to prevent this behaviour (see 4.2.1). This issue is related only to the version with motorised tilt for it is mounted to microscopes with two columns, ion and electron, and a sample needs to be tilted precisely between two planes in which lenses are focused.

This issue is important not because the number of occurrences but because it is undetectable until a stage is fully assembled and delivered to FEI. And repair then means dismantling significant part of the stage and possibility of distracting other parameters.

Repeatability

The problem of repeatability is described in 2.4. Note Table 5 where is a comparison of numbers of occurrences for each axis. There were almost twice as much issues with axis X than with axis Y. So it would seem that X axis is less stable at the first glance. But the most of these problems were caused by Y linear guide because any play and imprecision is transferred to the perpendicular axis. The new design which is meant to reduce these numbers is described in 4.2.2.

Drift

In the context of the stages a drift is an effect that occurs when stage still travels after finishing desired movement. There is a limit of 25nm/min defined by FEI standards. This problem appears to be related to stages linear guides and prestress of gearing. Further in this text a design upgrade is brought in.

Electronics

This category includes all failures of electrical components – encoders, feedthroughs and PCBs.

Other mechanical

All mechanical issues unrelated to repeatability, drift, Z-fall and leaking, that especially means problems with axes R and Z.

Other

This includes all other issues as well as refurbishing of old stages.

4.2. New design

Although there are many issues which would deserve attention, two of them have been chosen for their number of occurrences or (and, respectively) because of their impact on FEI's production. Looking at Table 4 it is obvious that the most important movement problem is repeatability. Chapter 4.2.2 is dedicated to the detailed description of the problem and to attempt to solve it.

The second most numerous issue caused by specific mechanical parts is falling in Z axis caused by play of tilt bearing. Urgency of this problem had been increased by need of finding an alternate type of bearing as a producer of the type used was about to cease its production.

4.2.1. Tilt bearing and flange

Some of 50mm stages suffer from so called Z-fall (see paragraph Z–fall above). The purpose of this design change is to provide solution to the particular problem as well as find replacement for old paired ball bearing.

The old solution has used back-to-back pared ball bearings 90x115x2.13 in tolerance class P5 according to DIN 620 [21]. They were fitted to a chamber door and secured by a simple flange (Picture 29).

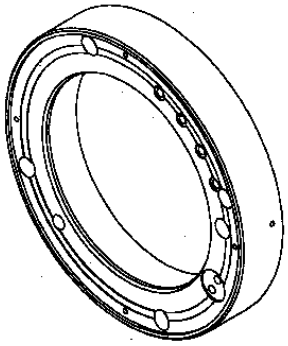

Picture 29 - old flange [22]

The old flange was attached by four M5 screws placed by 90°, all the other holes are used only with the stage version without motorised tilt (mounting end stop, scale etc.)
The first step to redesign tilt was to choose precise bearing which would be able to receive both radial and axial load and would have small play. There were no requirements about static or dynamic load or limit speeds because all the bearings in this category are highly overequipped in this regard.

The bearing that has been chosen eventually is SX011818 provided by INA. It is a crossed roller bearing which is perfect for a combined load. It does not have the best parameters available but also price had to be taken into consideration. And it also has one feature described later which made it interesting and worth-to-try.

Three new components have been designed – a flange consisting of an outer and an inner ring and a spacing ring to compensate the missing pair bearing. The whole new assembly is shown in Picture 30. It was essential to modify as little parts as possible so the new flange uses the same holes and has the same diameter as the old one.

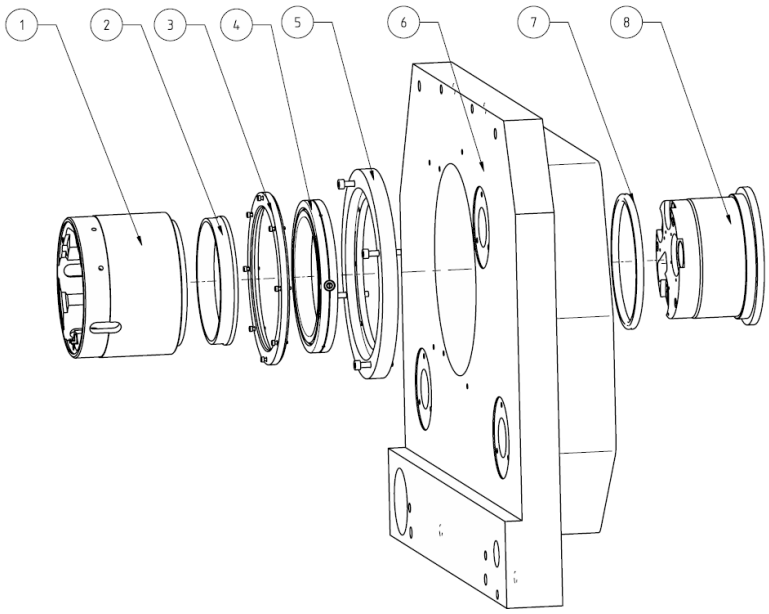

Picture 30 - new tilt assembly

ref.n.	part
1	outer tin
2	spacing ring
3	inner flange
4	bearing
5	outer flange
6	door
7	quad ring
8	inner tin

Table 6 - new tilt BOM

It is possible to see in Picture 32 how the new flange is arranged. Numbers of the positions correspond with Table 6 except for (9) which is quad-ring sealing. The key stone of the design is that the outer race of the bearing consists of two separate rings with a play in between (Picture 31).

The bearing (4) is tightly fitted to the inner tin (8) which is the actual moving part carrying the whole stage. The outer ring of the bearing is partially fitted to the chamber door (6) and to the outer flange (8) which are firmly bolted together. Then the inner part of the flange pushes bearing's outer race together evenly by eight M3 screws and thus makes it tighter. The cost for this is that that the bearing turns rather hard but that is not important as long as it within specified torque limit which is 5Nm

[23] and feedback loops works alright. It is unnecessary to consider warming or durability because a stage is tilted only few times a day.

Picture 31 - SX011818

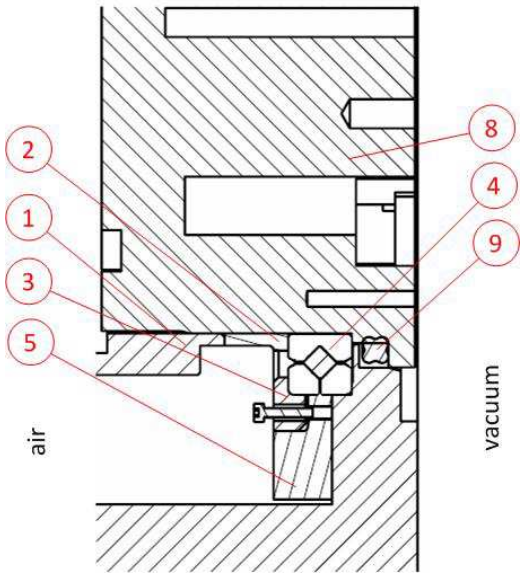

Picture 32 - new tilt assembly detail

This newly designed flange has been already used to successfully repair three stages with Z-fall issue. It is not enough cases for statistical evaluation but the solution has been proven viable.

4.2.2. Linear guides

As previously mentioned, the planar movements are carried on by the two chains composed of: DC motor – flexible coupling – encoder shaft – feed through with ball bearings - flexible coupling – threaded rod – (Y pulley) – linear guide (see Attachment 5). There is no meaning in changing motor or couplings. The first component worth considering would be the ball bearings in the flange but they are strained in radial direction and every error they could possibly cause would have to be in the perpendicular direction.

If the threaded rods were source of the repeatability problems it could be assumed that they would be of different character. The rods are prestressed by a spring and therefore the gear is tight. This means that, if there were any significant shape imperfections of the thread, movement error would be the same for every measurement while they are very irregular.

This leaves the last link of the kinematic chain which is the linear guide. Although there had been many problems with both axes X and Y, it has been decided to interfere only with axis Y at a time. It has been so for several reasons. First of all there have been more stages which had to be adjusted because of poor repeatability in X. It might seem to be paradox but in case when a guide is loose or imprecise it manifests in the perpendicular direction. This can be easily shown when a stage moves in only one axis. The other coordinate should be steady but it actually changes in tens of micrometres for Y movement and few microns while X moves. The much worse behaviour of the Y guide is likely caused by changing momentum strain from the snub pulley (see 2.3).

The redesigned part of the stage is in Picture 35. The redesign lies in replacing old linear guides with more precise and stiffer ones. Races of the old guides were composed of brass wires pressed into groove in dural. These grooves were milled out directly on X and Y slides and their complementary parts. This can be seen in Picture 33 where part of Y guide is. It is also obvious that the guide has only one ball as mentioned earlier.

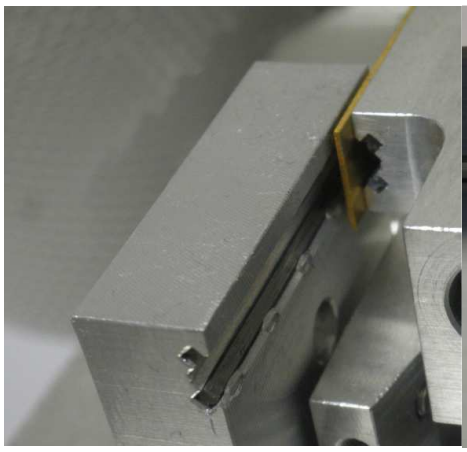

Picture 33 - old guide

Picture 34 - new guide

Guides used for redesign are crossed roller LWR3100 made by SKF group. They have every single parameter better than the old ones, for example the old guides had specified planeness to a horizontal base 0.1mm while the ones used for the new design have it 0.002mm [24] which is fifty times better.

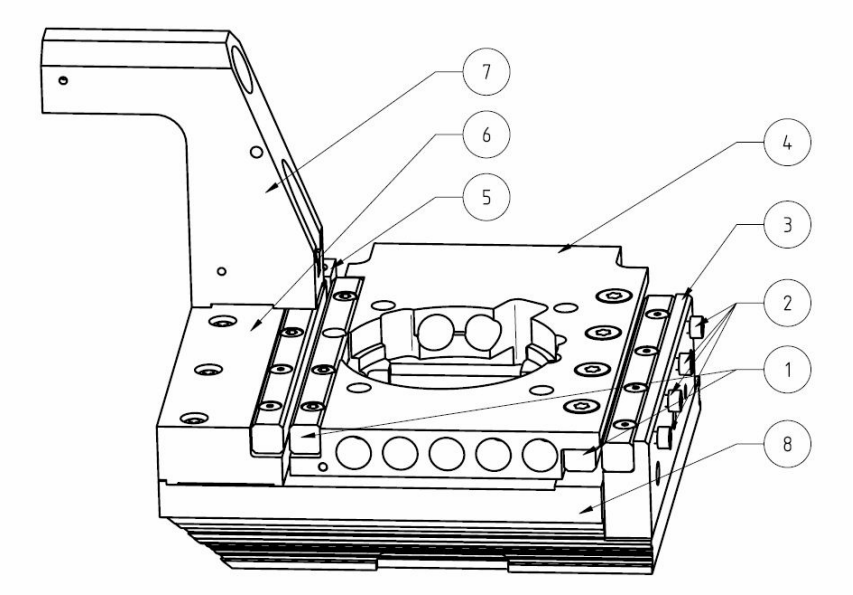

Picture 35- new linear guides assembly

ref.n.	part
1	linear guide
2	adj. screws
3	adj. Y guide
4	Y slide
5	stop block
6	Y guide block
7	X drive
8	X slide

Table 7- new linear guides BOM

So the assembly should bring improved precision of movement. Although it is definitely important the main issue was that guides were stiff enough. It is shown in Picture 34 that LWR3100 has long roller cage which should provide more stable behaviour of Y slide than just two flexible fitted balls.

The whole new assembly is in Picture 35. Changing the guides meant to fit pre-manufactured LWR3100, instead the old ones which were grooved into the slide and adjacent parts, without changing outer dimensions of the assembly so it could be mounted into otherwise unmodified stage. The most difficulties came from the fact that the new guides are relatively large compared to the rest of the parts and the stage was dense structure already with almost no space left. It resulted into remodelling six parts and creating two new components.

LWR3100 has fitting specified in manual [24] however, they were not adhered for the assembly in attempt to lower price of the component. Measurements of redesigned stage are summarized and evaluated in 0.

Vacuum compatibility

There is one specific and important feature when designing microscope stages or parts placed inside vacuum chamber in general. The most of common industrial plastic components and greases contains various chemical additives (such as plasticizers) that evaporate under high vacuum and thus they degrade it. The main problem, which might be the obvious guess, is not that these free particles would interfere with scanning

electrons' trajectory but something different. When molecules get into proximity of a sample they are ionized by the electron beam and then they chemically bond to the sample's surface and devalue it.

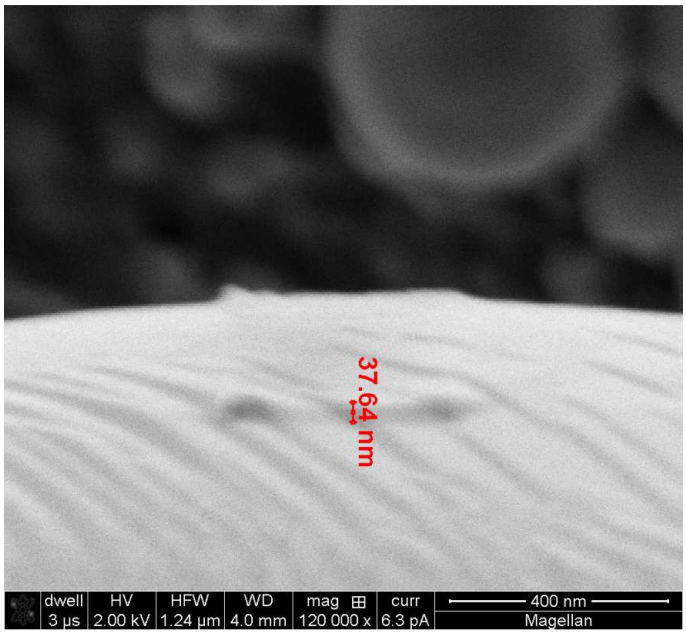

Picture 36 - contamination measurement

The cage which is part of LWR3100 guides is made of unspecified (by distributor) plastic and thus vacuum contamination must be taken into consideration. The two cages were placed into a previously plasma cleaned microscope chamber for the empirically verified period of 24 hours and then the contamination was measured by prescribed FEI procedure. It says to scan a square field 400x400nm at the edge of a tin ball of 10 µm diameter for 10 minutes. The sample is the same as for the repeatability measurement. The resolution is 1024x768 and dwell time 1µs (per pixel) [4].

During this procedure a square structure of formerly free molecules grows in the field of view (Picture 36 – dwell time is different to improve the picture quality). Its height corresponds with the level of contamination and it is the measured value.

Five measurements were done because the height of the grown structure depends also dependant on quality of beam focus and proximity of other tin balls on a sample. All the results were in interval from 35nm to 40nm while limit specified for Quanta microscopes is 50nm. So the standard LWR plastic cages can be used without modification.

4.2.3. Snub pulley

The snub pulley is an important component which transmits rotary movement of the Y lever to linear motion of the stage. Therefore it directly inflicts the accuracy and repeatability of a stage. In the Picture 37 there is a comparison of the old design and the new one brought in this thesis. The merit of the change is replacing a loose single bearing (3) at the end of the arm (1) with paired ones (5). All the deep groove ball bearings are of the same size 4x11x4. There is a serious lack of choice of these on the market and what is more important all the types offered are meant for completely different use than FEI needs. They are designed for high speed appliances it means that they have big play because of the heat generation. None of the major manufacturers provides bearings that would fit microscope stage's requirements. The original 50mm stage's designer solved this problem by using face to face arrangement of the bearings. However, it has been done only with one pair for an unknown reason. So the neglected fit of the remaining bearing (3) is the real drawback of the old design. And the other issue would be that the bearing is attached by a standard screw M3 with countersink head (4) which is utterly insufficient.

The redesign lies in using paired bearings in both cases and mounting them with a custom screw so the whole fit would be tighter. This also required new shape of the lever (6) and the stage's bridge had to be worked down a little (see Attachment 4). This should provide more stable behaviour of the stage.

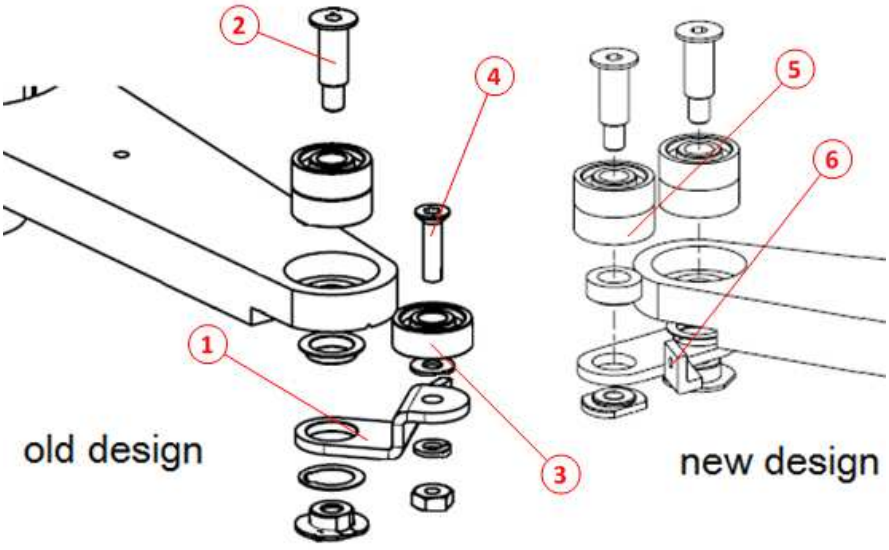

Picture 37 - snub pulley

5. Stage movement analysis and test-tool's analysis

Two stage's movement parameters have been analysed – overall accuracy and repeatability. Difference between these and their relation has been explained in 2.4.

All measurements performed by the test-tool had been compared to measurements which have been done by a microscope. This has been done in order to obtain statistical characteristics of the device and distinguish them from statistical characteristics (random behaviour) of a stage itself. An electron microscope can be considered to be many times more precise gauge than any other kind but it is still necessary to evaluate standard FEI measurement procedure. The most proper way of doing this would be to compare results of the measurements with a known etalon. Regrettably this was not possible due to lack of proper samples of precise enough dimensions. However, the procedure consists of two parts which can be evaluated separately – acquiring SEM image and image processing which follows. It is very difficult to enumerate errors in electron microscope images. But it is reasonable to assume that these errors would be negligible regarding the fact that a microscope uses about one hundredth of its possible magnification during the test.

Because a result of the image processing routine are displacements in axes X and Y it is possible to feed it with images with defined relative positions and compare these with the results of computation. This was done in the simplest way possible – a single image has been used for all the steps which correspond with displacement of 0. This was also result of image processing up to sixth decimal place in microns.

With respect to the previous paragraph it is possible to considers FEI's measurement an etalon and compare other results with it.

5.1. Measurements

The meaning of the measurements and statistics described below is to provide basis for comparison of the old and new stages design regarding its accuracy and movement repeatability. Evaluation of the old design had been done by a Quanta FEG microscope and so, as mentioned above, measurements errors are negligible and measurements represent real behaviour of the stage. All measurements were performed on the same stage unless said otherwise. Due to the small amount of stages available and protracted character of the measurement it was not possible to test statistically significant number

of mechanisms. So the results are only informative but they serve their purpose which is to determine whether the redesigned stage performs markedly better and is worth further development.

In the following paragraphs there are separately compared the results of the old and the redesigned stage for of each parameter and axis.

5.1.1. Accuracy

The standard way to measure movement's accuracy at FEI is to determine position of calibrated 70µm crosses (Picture 38) spaced by 5mm in a matrix on a silicon wafer (as part of more complex patterns - Picture 39). So at the beginning the middle cross had been aligned to the centre of the image and a stage made 5mm steps separately in axes X and Y. The accuracy of the movements is determined by deviation of the cross from the image's centre.

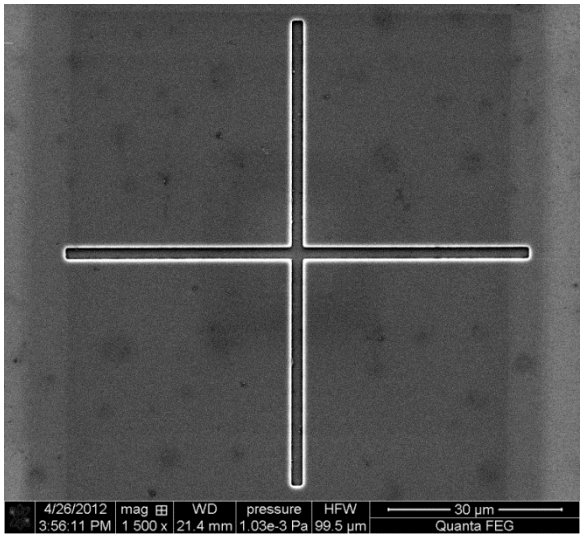

Picture 38 - cross on a wafer

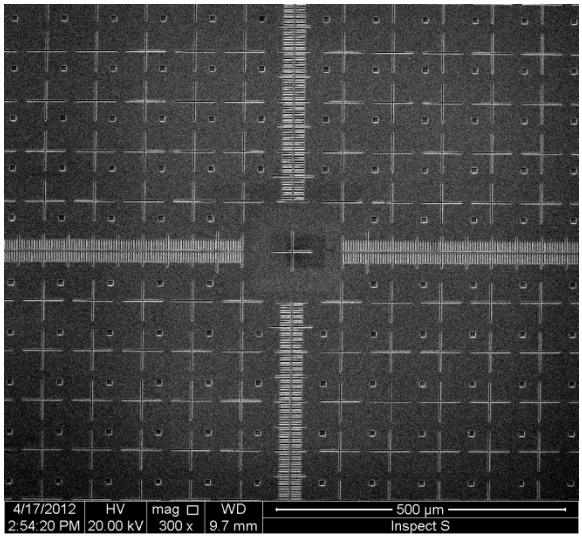

Picture 39 - wafer

This test is performed at FEI's high end stages, it is fully automated and every cross of the matrix is checked. It cannot be done with 50mm stages for three reasons. First, stage's rotation control is not precise enough to align a wafer with the image and it is difficult to do so manually. Second, a manually tilted stage is never precisely horizontal and image has to be refocused during movement in Y. And the third reason is that the movement in XY plane is not precise enough and summed up error could cause that the desired cross would not be in the view at all.

So the accuracy test has been performed manually in a simplified way. The stage was moving in only one axis at a time with step of 5mm. Both axes were measured separately.

In each step a picture was acquired and then evaluated by script made in NI Vision Builder using geometry comparison methods and filtering. Picture 40 should demonstrate basic idea of the script – filtering the first image and finding the centre of the cross, then doing the same with the image acquired in the following step. The result of the script is the length of the vector connecting the centres of the crosses and its counter-clockwise angle to the horizontal axis.

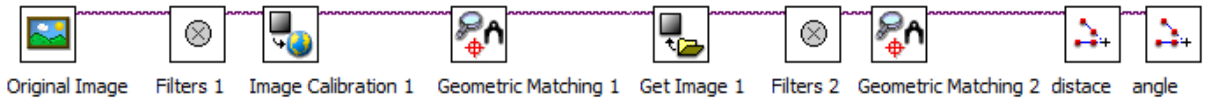

Picture 40 - cross detection

Magnification was set to 1500x which theoretically provides resolution of the measurement approximately 0.09µm if there was no distortion and each cross had absolutely sharp edges.

The measurement started with an old-design stage. The stage was adjusted to satisfy repeatability criteria and then tested in axis X. However, the first results proven right the third reason mentioned earlier. Deflection in each step was so big that it made the measuring method inapplicable. A cross could not be found in the field of view after three 5mm steps. The deviation was estimated to be approximately 20-30µm, which is still within allowed limits although (see Table 1). The deflection had character of one sided positive offset added to each step – each step was about 20 µm longer than 5mm but with only little dispersion.

The behaviour of the stage could be adjusted by setting the flexible fit (thus pressure) of the linear guide (see 2.3).Table 8 shows example data measured for one specific adjustment of X guide. The deflections in the table are all positive and the differences in the second row are between two following steps.

step	**1**	**2**	**3**	**4**	**5**
deflection [µm]	24.6	22.3	25.3	26.9	23.2
difference [µm]	-	-2.3	3.0	1.6	-3.7

Table 8 - axis X deflections

The offset could even be made of opposite direction. So it might seem that the stage could be easily set to operate without this offset. But the problem was that tightness of the X guide influenced repeatability results of both axes, X as well as the perpendicular axis Y (described later). And when the linear guide X became too loose the stage deflected also in axis Y.

Axis Y manifested very similar behaviour to axis X. It is clearly visible in Picture 41 which demonstrates deflection in two consequent movements in axis Y. The right image has half magnification to show the real position with respect to the initial cross which is highlighted on the top. Please note that every cross has spread of 70µm. It can be seen that deflection had the same orientation roughly the same magnitude.

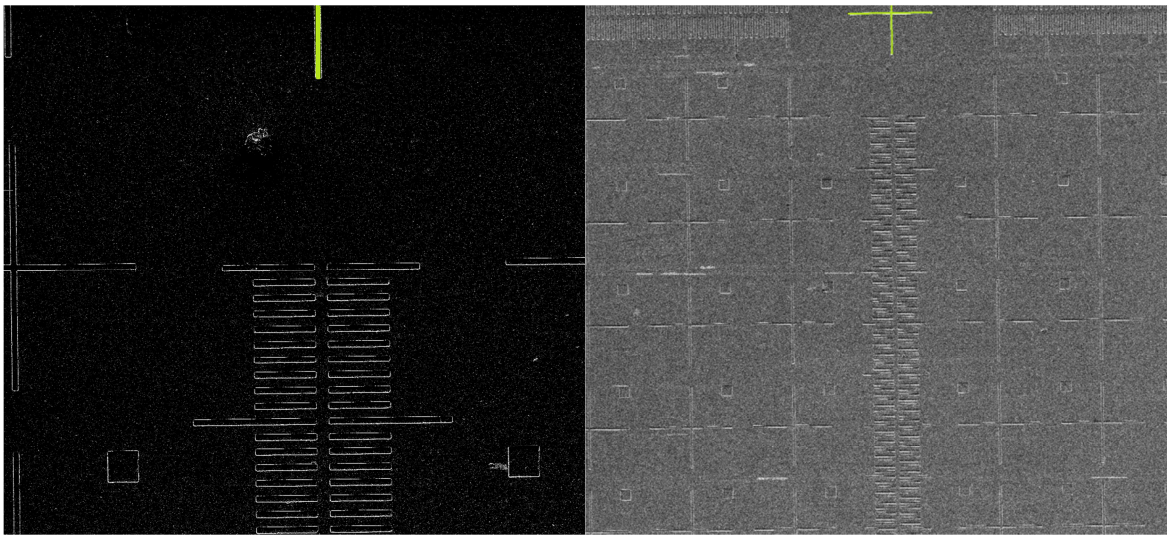

Picture 41 - Y deflection

The conclusion based on these measurements can be defined as follows. Magnitude and orientation of deflection of point to point movement in plane XY is highly dependent on pressure in linear guides. However, spread of the magnitude is stable and is not influenced by setting of the guides.

The redesigned stage was tested in the same manner. Because axis X remained unchanged also its characteristics were very similar to the original stage and the results are not further mentioned. The only difference is described in detail in 5.1.2 about repeatability.

However, results of the modified axis Y (see 4.2) are different. This was the only axis actually measurable by the desired method. The prototype stage made set of 32 steps in the whole range of axis Y while X coordinate was set to 0. Table 9 shows results of the measurement of the new stage. The numbers in each step are perpendicular projections of deflection from the desired position. All the deflections are deep within the limits.

step	**1**	**2**	**3**	**4**	**5**	**6**	**7**	**8**	**9**	**10**	**11**	**12**	**13**	**14**	**15**	**16**
$X_{[\mu m]}$	-0.52	-1.23	0.32	-5.04	-0.92	2.01	1.54	0.94	-3.58	2.78	2.78	0.20	1.70	1.13	0.82	-2.25
$Y_{[\mu m]}$	0.32	0.84	-0.88	0.42	-0.27	-0.34	1.96	-1.66	0.40	1.95	1.36	-1.76	0.56	1.81	0.94	-2.50
step	**17**	**18**	**19**	**20**	**21**	**22**	**23**	**24**	**25**	**26**	**27**	**28**	**29**	**30**	**31**	**32**
$X_{[\mu m]}$	-0.64	-1.15	-3.01	-0.61	1.01	2.10	-0.36	-0.76	-1.97	2.92	-1.23	0.31	3.73	0.97	0.90	-1.23
$Y_{[\mu m]}$	-0.44	-0.29	2.46	-2.33	0.16	-0.42	1.92	-1.70	0.63	-0.14	0.98	-1.67	2.85	1.75	1.00	-3.92

$\overline{X}_{[\mu m]}$	**0.052**	$\overline{\lvert X \rvert}_{[\mu m]}$	**1.984**	**relative deviation X**	**0.032%**
$\overline{Y}_{[\mu m]}$	**0.125**	$\overline{\lvert Y \rvert}_{[\mu m]}$	**1.585**	**relative deviation Y**	**0.025%**

Table 9 - new stage accuracy X

There are several other things that can be observed from the data. The average error in both axes is close to zero, **without significant offset to neither direction**. It means that the stage is well adjusted and the linear guides are well aligned. However, a microscope user is more interested in absolute magnitude of the error rather than its average. The stage performed well also in this. Absolute averages for both axes shown in Table 9 are within limits. Even the error with the biggest magnitude (step 4, axis X) was -5.04µm which means relative deviation of 0.1%, tenth of the specified limit.

These results were achieved independently on setting of X guide and with new Y linear guide tightly screwed to its bedding. It means that accuracy of the redesigned Y axis is not influenced by subtle adjustment of the spring-washer fit like the old one was but only by compliance of dimension and geometric tolerances. Improved accuracy parameters in Y movement can be also partly attributed to modified snub pulley with lesser radial play.

5.1.2. Repeatability

One of the problems known from the 50mm stages production is that the results of repeatability test, under the same conditions, vary. So the aim of the following statistics is to determine credibility of such measurements, “repeatability of repeatability test” respectively.

A set of 71 repeatability measurements has been performed at one stage of the old design, the same number at the prototype stage and results are as follows. The measurements were made in standard Quanta FEG microscope as described in 2.5 and 5. All values in following figures are in [µm].

A histogram of results for axis X in Figure 1 compares acquired values with step of 0.1µm. It could be told that results of the prototype are slightly better because about 75% of the values are in range of 0.2µm while the old stage had the same part spread across 0.3µm. But more can be told on base of statistic characteristics of the data.

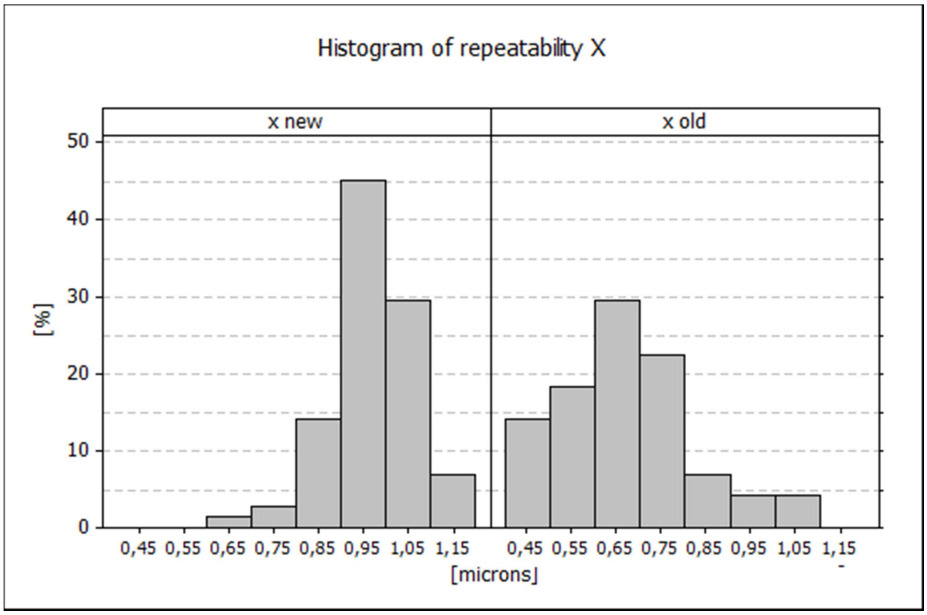

Figure 1 - repeatability X histogram

The first thing to do with data measured is to test whether they have normal distribution or not so the null hypothesis had to be tested. The criteria used to decide that was Anderson – Darling test with confidence interval 95%.

Resulting P-value for the prototype’s data was 0.46 and for the old stage is was 0.26 so in neither case the null hypothesis was rejected and data can be considered

normally distributed. It means that statistical moments mean and standard deviation can be calculated. Basic statistic characteristic can be found in Table 10.

	old design	**new design**
mean [µm]	0.67	0.97
standard deviation [µm]	0.15	0.10
median [µm]	0.66	0.96
inter-quartile range [µm]	0.21	0.13
maximum [µm]	1.10	1.18
minimum [µm]	0.34	0.67

Table 10 - statistics for axis X

Both stages performed extraordinary well and mean and median values are deep within the limit. Average repeatability value known from production for the old design is 1.9µm [4]. What is more of a concern are spreads of the measured values represented by standard deviation or inter-quartile range. Even though that prototype stage reached 50% smaller standard deviation, its value is still the same order as of the old design.

The same measurements were done for axis Y. Histogram shown in Figure 2 illustrates distribution of the results. It is obvious that the prototype was not very well adjusted compared to the other stage but it still performed within limit. So it can be stated that, regarding repeatability, the modified stage is at least equivalent to the standard design.

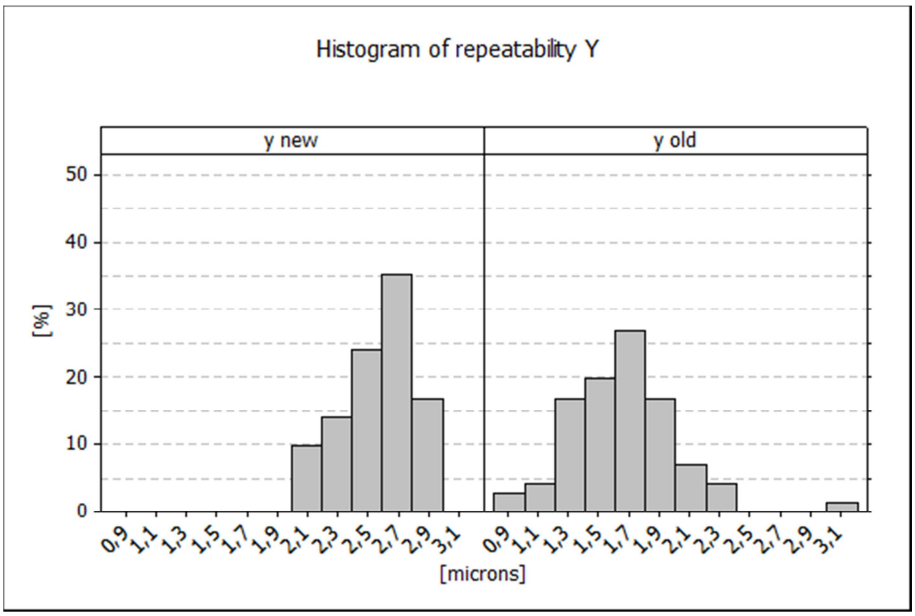

Figure 2 - repeatability Y histogram

Measured data was processed the same way also for Y axes. P-value of the old-stage dataset was 0.38 and so the data can be considered normal at confidence interval 95%. However, in the case of the new stage the P-value was less than 0.05 and the null hypothesis had to be rejected. It could be caused by some non-normal noise during the measurement or simply by insufficient number of samples. Nonetheless mean and standard deviation were calculated for both cases but not much of importance should be attached to it in this particular case. Inter-quartile range is more of the importance. The results are summarized in Table 11. The prototype had again smaller spread of results but due to relatively low number of measurements it is not distinctive enough to be conclusive.

	old design	**new design**
mean [µm]	1.66	2.58
standard deviation [µm]	0.34	0.24
median [µm]	1.65	2.60
inter-quartile range [µm]	0.43	0.33
maximum [µm]	3.07	2.96
minimum [µm]	0.95	2.01

Table 11 - statistics for axis Y

Standard deviations of the same order as the measured quantity makes repeatability testing, as it is currently done, unreliable. It would be reasonable to reconsider measurement evaluation so the statistic parameters of the stages were taken into consideration.

A relation between repeatability of one axis and adjustment of the other is mentioned in 5.1.1. To illustrate this, a simple experiment has been carried out. Repeatability was measured for various settings of X guide. The screws prestressing the spring washers which are pushing the guide were tightened in small steps simultaneously. The 10 steps in Table 12 are evenly spread over two turns of the screws. There was no better way to represent the pressure in the guide because no torque wrench was available.

Old design

step	$3\sigma_X$ [µm]	$3\sigma_Y$ [µm]
1	3.53	3.28
2	2.50	2.77
3	2.62	2.38
4	2.68	2.87
5	2.89	2.01
6	2.77	2. 7
7	3.09	2.74
8	3.68	2.71
9	4.21	2.52
10	4.86	3.58

New design

step	$3\sigma_X$ [µm]	$3\sigma_Y$ [µm]
1	0.99	3.42
2	1.01	3.73
3	0.95	3,26
4	1.02	2.58
5	1.06	2.03
6	0.97	1.72
7	1.13	1.86
8	0.97	2.58
9	1 08	2.87
10	1.18	2.39

Table 12 - axis repeatability relation

The data for the old design show that there certainly is relation between adjustments of the X and Y linear guides, however, not a simple one. It is obvious that balance exists between too tight and too loose setting of the stress. When the guide is too tight every roughness on the surface of the race can manifest undamped in both X and Y directions. When it is too loose, prestressing simply ceases to serve its purpose.

However, values measured at the prototype are different. While $3\sigma_y$ changed in the similar manner as in the previous case, $3\sigma_x$ stayed constant within the range of its standard deviation. There are two things that can be assumed from this result. First, stress in a linear guide influences repeatability of movement in its own axis as well as in the perpendicular one. And second, thanks to its stiff fit the new linear guide is resistive to changes of stress in X guide. It allows separating settings of the linear guides and thus it makes the stage much easier adjustable.

It is necessary to consider Table 12 with caution with respect to statistical characteristics of the 50 mm DC stages. Figure 3 depicts Table 12 as dependency between repeatability values in axes X and Y for the old and new design of the stage. The conclusions deduced in the previous paragraphs can be clearly observed.

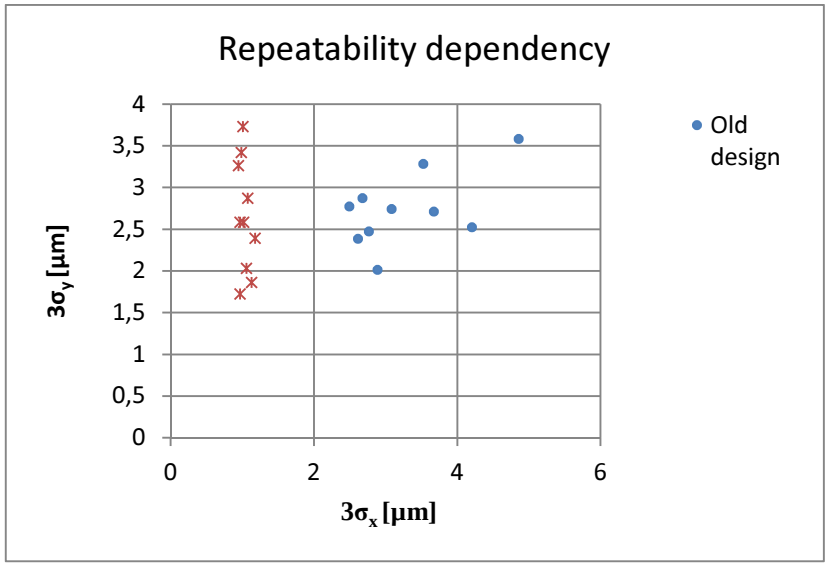

Figure 3- repeatability dependency

Change of the linear guides and modification of the snub pulley brought some positive changes. Although it did not provide desired decrease of spread of repeatability results it improved accuracy in axis Y and significantly raised its stability and stiffness. It also allowed separation of axes setting and thus made stage's tuning up easier. And another important asset is shortening of manufacturing process of modified parts which fully compensates price of purchased LWR 3100.

5.1.3. Test tool measurement and characteristics

Mechanical and hardware part of the measuring device have been already described so the last part remaining now is to determine its accuracy and suitability. There are two types of sensors used – linear quadrature encoders and laser triangular sensors.

The encoders have resolution (step) of 0.1µm [7]. Every encoder has some quantisation noise and this uncertainty is represented by uniform probability distribution [25] which is shown in Figure 4, where *s* is encoders step – resolution.

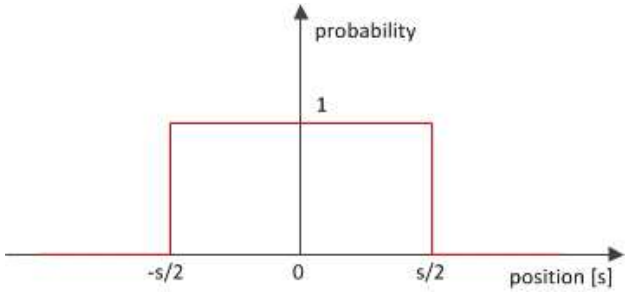

Figure 4 - encoder probability

Uncertainty of measurement with a sensor with such noise is [26]:

$$u = \frac{\Delta}{\tau} \tag{4}$$

$$u_E = ku \tag{5}$$

Where u is uncertainty, τ is a coefficient specific for a type of distribution, in this case $\sqrt{3}$ [26] . And Δ is maximal error of the sensor which is half of the encoder's step, 0.05µm.Term k is expansion factor, its value is $\sqrt{3}$ for uniform distribution [26]. So after putting these values to equation (4) and (5), resulting uncertainty u_E equals:

$$u_E = \sqrt{3}\frac{0.05\mu m}{\sqrt{3}} = 0.05\mu m \tag{5}$$

It is overall uncertainty for measurements in axis Y. But in axis X there are two displacements measured (see 3.2 and 3.4) and the results are added up.

The laser sensor has also resolution 0.1µm. Its range is 2mm and linearity of the transducer is 0.1% [13]. Because measured data never exceed range of units of microns (thousandths of the range), errors caused by nonlinearity can be neglected. Uncertainty of measurement was calculated on basis of acquired data sample. In real functioning the laser returns moving average of last 128 acquisitions with rate 324.4Hz. A corresponding data set was evaluated. The sensor was set to return non-averaged measurements at the same frequency for 0.4s to get 128 samples. Assuming normal distribution of the noise, uncertainty is calculated as standard deviation [26] so, using equations (3) and (4), laser measurement uncertainty u_L is:

$$u_L = \sqrt{\frac{1}{n}\sum_{i=1}^{n}(\tilde{x}_i - \mu)^2} = 0.0023\mu m \tag{6}$$

And overall uncertainty for axis X is calculated as sum of squared of u_L and u_E [26]:

$$u_X = \sqrt{u_L^2 + u_E^2} = \sqrt{0.0500^2 + 0.0023^2} = 0.05012 \tag{7}$$

Because measurement uncertainty must be rounded to the first significant digit:

$$u_E = u_L = 0.05\mu m \quad (8)$$

Before the device was implemented at stage manufacturer's plant, the same set of measurements as in previous case with a microscope was performed to prove whether it provides relevant data. Unfortunately it was not possible to measure the very same stage but Table 13 shows that spread of values is comparable and may represent stage's behaviour.

Test tool results

	X	**Y**
mean [µm]	1.32	1.76
standard deviation [µm]	0.15	0.19
median [µm]	1.32	1.73
inter-quartile range [µm]	0.28	0.30
maximum [µm]	1.73	2.18
minimum [µm]	1.01	1.35

Table 13 - test tool results

Use of the device has brought decrease in number of stages which do not pass repeatability measurement at FEI down from 10 - 12 a month before implementation to 1 – 3 a month since August 2011 [4]. The fact that some stages are still not caught up by the test tool may be caused by unstable conditions under which the test are conducted. Likely reason is changing temperature in a non-air conditioned room in which the stages are made and measured. Resulting size dilatations of mechanical part can be in order of tenths of millimetres which can change stage's behaviour considerably.

6. Conclusion

It is possible to say that all the goals of this thesis were reached to a satisfactory degree along with some additional improvements that resulted from the project.

Literature search part provides overall review of possibilities of electron microscope stage motion repeatability measurement. The most suitable was chosen for practical implementation from those. The created measuring device brought significant decrease in number of stages that had to be reclaimed due to repeatability. Although that it did not eliminate reclaims completely it can be considered success. The factors which cause that some results are different at stage manufacturer and at FEI are yet to be identified and corrected.

Based on production database search and knowledge of stage's mechanics, weak spots of the old stage design were discovered - movement repeatability instability and so called Z-fall issue. These problems were used as a basis for design changes of the mechanism and three modifications were made – two related to repeatability and one to Z-fall.

Z–fall issue was successfully solved by bearing replacement and new composed flange which makes advantage of the new bearing's split outer run. The design change was used to repair stages where Z-fall issue occurred with success.

Design changes related to repeatability were change of principle of linear guides in axis Y and modification of the snub pulley. Both were implemented into a prototype which was consequently measured and its result compared with the old version of the stage. The modified stage was fully functional. Data of the measurement has shown that unfortunately stability of repeatability results was not improved but the new design has some other benefits. Accuracy in axis Y was improved. Also the prototype allows both axes X and Y to be adjusted without influencing each other, which was not possible with the old stage. And last but not least shortens stage's manufacturing process while keeping the price the same.

Literature

[1] FEI company, “FEI,” 2012. [Online]. Available: www.fei.com. [Accessed 1. 3. 2012].

[2] A. M. Davidson M.W., Encyclopedia of imagining science and technology, Online ISBN: 9780471443391, 2002.

[3] FEI company, Introduction to electron microscopy, ISBN 978 0 578 06276 1, 2010.

[4] FEI, *FINAL Test, production database system,* 2012.

[5] FEI comany, *Motorstage repeatability measurement,* 2009.

[6] Micro-Epsilon, *High resolution capacitive displacement sensors and systems.*, Ortneburg, Germany, 2011.

[7] Renishaw, “RGH24 series readhead datasheet,” 2004.

[8] Renishaw, “RGH24 linear encoder system,” [Online]. Available: http://www.renishaw.com/en/rgh24-linear-encoder-system--6444. [Accessed 1. 3. 2012].

[9] C.F.Lepple, *Implementation of a High-speed Sinusoidal Encoder Interpolation System,* Virginia Polytechnic Institute and State University, 2004.

[10] Heidenhain, “Heidenhain - measuring principles,” [Online]. Available: http://content.heidenhain.de/presentation/basics/en/index.html. [Accessed 4. 3. 2012].

[11] Renishaw, “RGS20-S, RGS20-PC, RGS40-S, RGS40-PC scale datasheet,” 2008.

[12] Micro Epsilon, “Micro Epsilon glossary,” [Online]. Available: http://www.micro-epsilon.cz/glossar/Laser-Triangulation.html. [Accessed 5. 3. 2012].

[13] Micro Epsilon, “Laser Triangulation Displacement Sensors,” 2011.

[14] Micro Espilon, “Instruction Manual optoNCDT 1700,” 2011.

[15] Rexroth Bosch Group, “Rexroth NYCe4000 - Hardware system manual,” 2007.

[16] ESSA, “IEPC RS manual”.

[17] U. M. d. N. M. Pavelka M., *XTLib interface descripion for third party developers,* FEI, 2011.

[18] Micro Epsilon, “Micro Espilon industrial manual - Data Acquisition Library,” Ortenburg, 2011.

[19] Microsoft, “Microsoft support - What is a DLL,” 4. 12. 2007. [Online]. Available: http://support.microsoft.com/kb/815065. [Accessed 3. 1. 2012].

[20] National Instruments, “Using .NET with LabVIEW,” 8. 2007. [Online]. Available: http://zone.ni.com/reference/en-XX/help/371361D-01/lvconcepts/using__net_with_labview/. [Accessed 5. 4. 2012].

[21] Philips, “Philips 4022 198 14811,” 1988.

[22] Philips, “Philips 4022 197 54035,” 1988.

[23] FEI, *4022 293 30983 - 160-01,* 2012.

[24] SKF , “Precision rail guides,” Schweinfurt, 2004.

[25] D. J. T. M. J. Kelly, “Overcoming encoder quantisation noise in an adaptive position controler,” *International journal of Machine tools and Manufacture,* 2000 / 40.

[26] J. J, “Merici technika I,” 2007. [Online]. Available: http://rss-m.fm.tul.cz/course/mt1m.htm. [Accessed 5. 15. 2012].

List of pictures

List of tables

List of figures

List of attachments

Printed

1. **Measurement tool assembly**
2. **Part Number 1021223** – tilt change assembly drawing
3. **Part Number 1023134** – linear guides change assembly drawing
4. **Part Number 1016365** – snub pulley change assembly drawing
5. **Stage kinematic chain** – section view

On appended CD

1. **Compiled measurement program** and used dynamic libraries
   - folder *"root\compiled\..."*
2. **Measurement tool drawings**
   - drawings of components of the measurement tool
   - folder *"root\draw\tool\..."*, files named according to printed attachment 1
3. **Tilt flange drawings**
   - drawings of components of the tilt flange assembly
   - folder *"root\draw\tilt\..."*, files named according to printed attachment 2
4. **Linear guides change drawings**
   - drawings of components related to the change of linear guides
   - folder *"root\draw\guides\..."*, files named according to printed attachment 3
5. **Snub pulley drawings**
   - drawings of components related to the change of linear guides
   - folder *"root\draw\pull\..."*, files named according to printed attachment 3
6. **Repeatability data**
   - Minitab file with measured repeatability data from 5.1.2
   - file *"root\data\repeatability.mpj."*

7. **Accuracy data**
    - images acquired for prototype Y accuracy measurement
    - folder *"root\data\accuracy"*
8. **Datasheets**
    - datasheet of Renishaw RGH24Y
    - bearing SX011818A
    - linear guider SKF LWR3100
    - datasheet and user manual of Micro-Epsilon ILD1700-2
    - folder *"root\datasheets*

Attachment 1

Measurement tool assembly

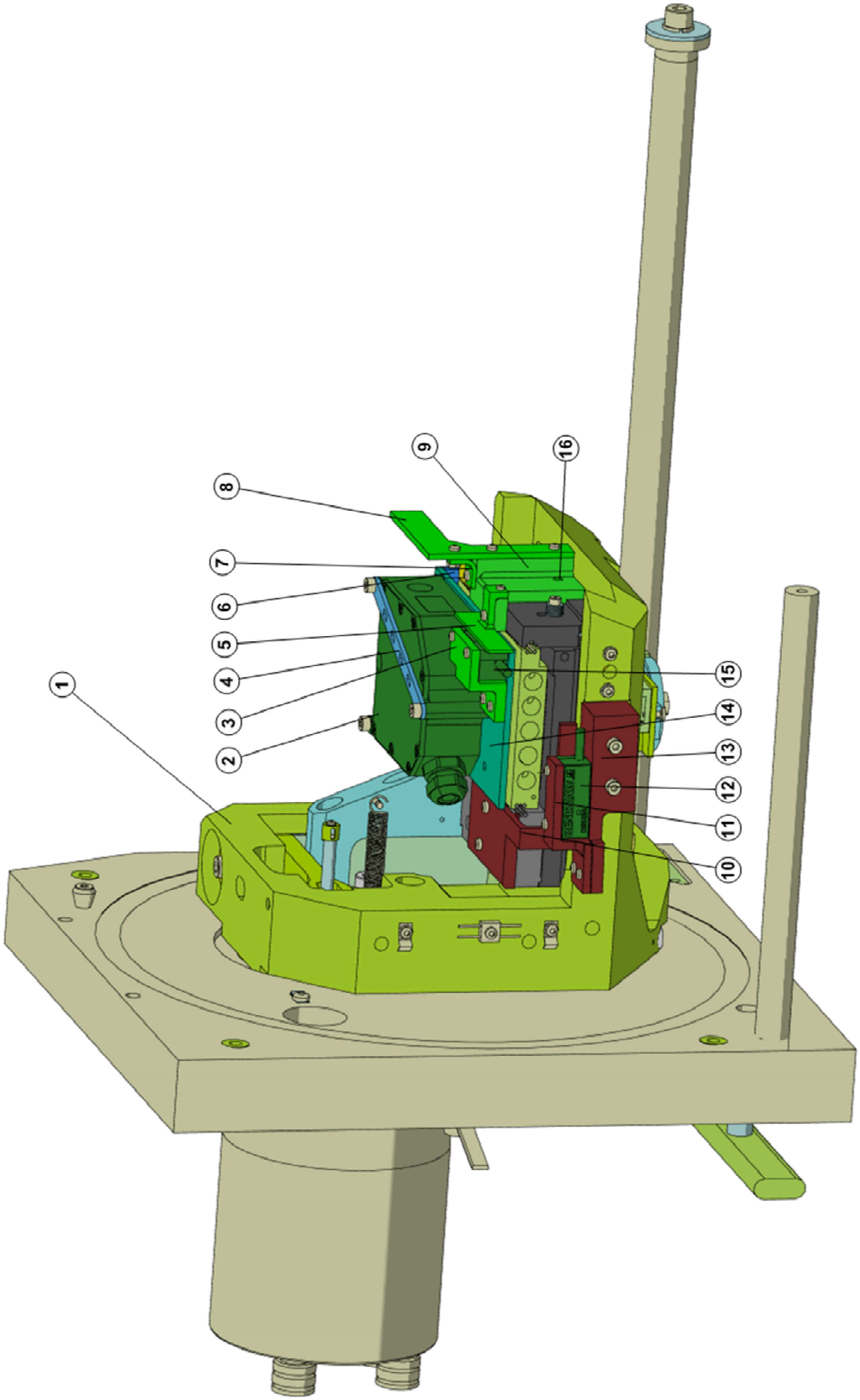

Bill of material

Pos.	Name	NC
1	50mm DC stage	4022 293 36541
2	Laser sensor ILD 1700-2	
3	Y encoder holder	1020867
4	Cable holder	1018677
5	Y scale	1018708
6	Y align	1018653
7	Y angle	1018715
8	Laser ruler	1018712
9	Y main block	1018681
10	X scale	1019758
11	X encoder holder	1020869
12	Encoder RGH24Y	
13	X holder	1018659
14	Baseplate	1018327
15	Encoder RGH24Y	
16	Y pin	1018717

REV	DATE	ECR	DESCRIPTION OF CHANGE	NAME
A	21-May-2012			Vaske, Frantisek

ATTACHMENT 2

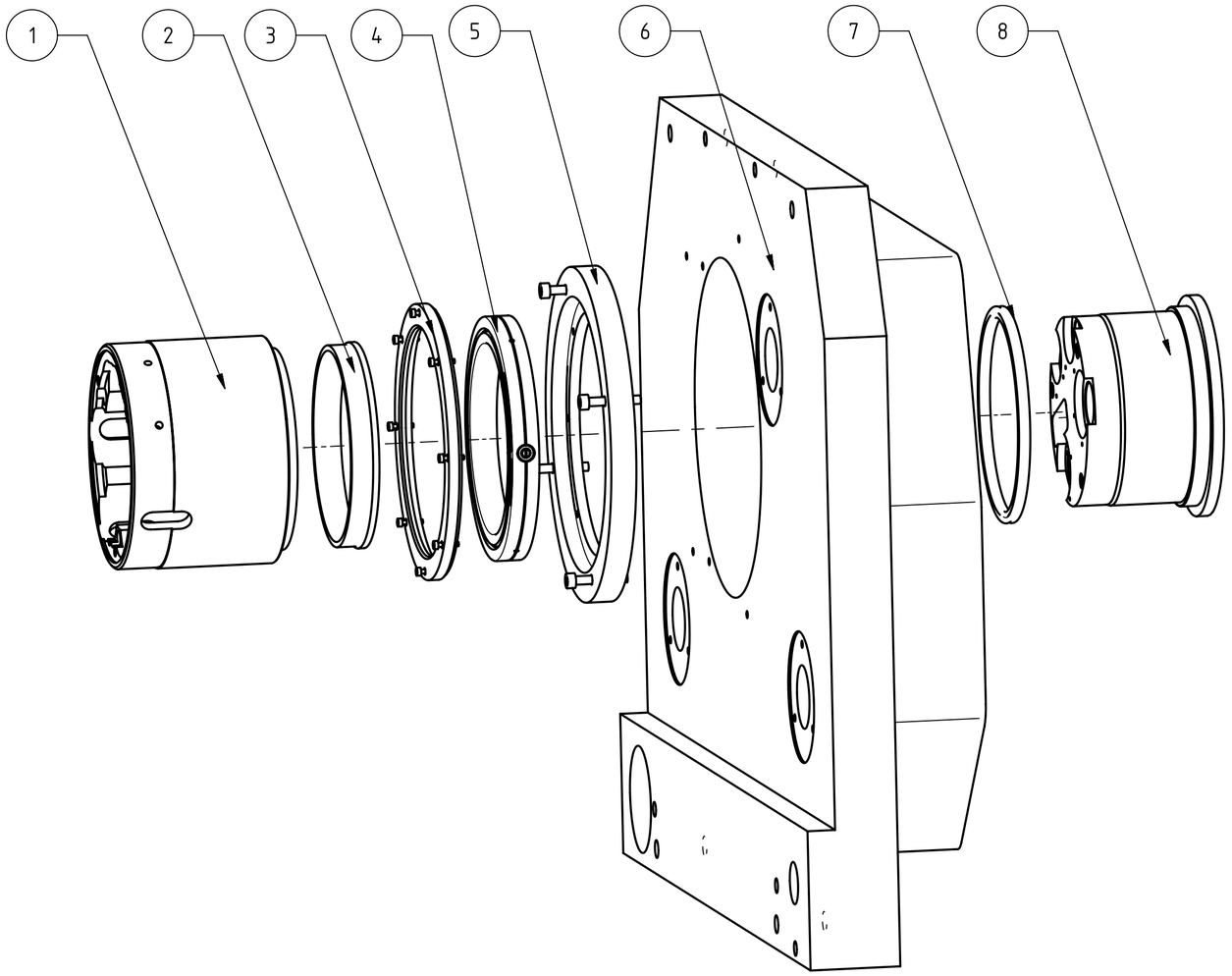

8	4022 260 17893	1	INNER TIN	
7	4022 198 14722	1	QUAND RINNG	
6	4022 260 53974	1	CHAMBER DOOR	
5	1021219	1	OUTER FLANGE	CD - DRAW\TILT\1021219
4		1	BEARING	SX011818A
3	1021237	1	INNER FLANGE	CD - DRAW\TILT\1021237
2	1021234	1	POS. RING	CD - DRAW\TILT\1021234
1	4022 260 53982	1	OUTER TIN	
POS	NC	N	NAME	NOTE

THIRD ANGLE PROJECTION

FEI

PREDECESSOR: | REVISION:

GENERAL ROUGHNESS: - Ra in µm

MATERIAL:

STATUS:

SCALE: NTS

TREATMENT:

NAME: Vaske, Frantisek

SIZE: A2

SHEET BIRTH DATE: 21-May-2012

UNIT: mm

TITLE: TILT ASSEMBLY

PART NUMBER: 1021223

REVISION: A

DRAWN ACCORDING TO: QEO-11-010

FILE TYPE: ☑

LOCATION: BRNO

SHEET NAME: Physical data

SHEET 110-01 OF 01

REV	DATE	ECR	DESCRIPTION OF CHANGE	NAME
A	21-May-2012			Vaske, Frantisek

ATTACHMENT 3

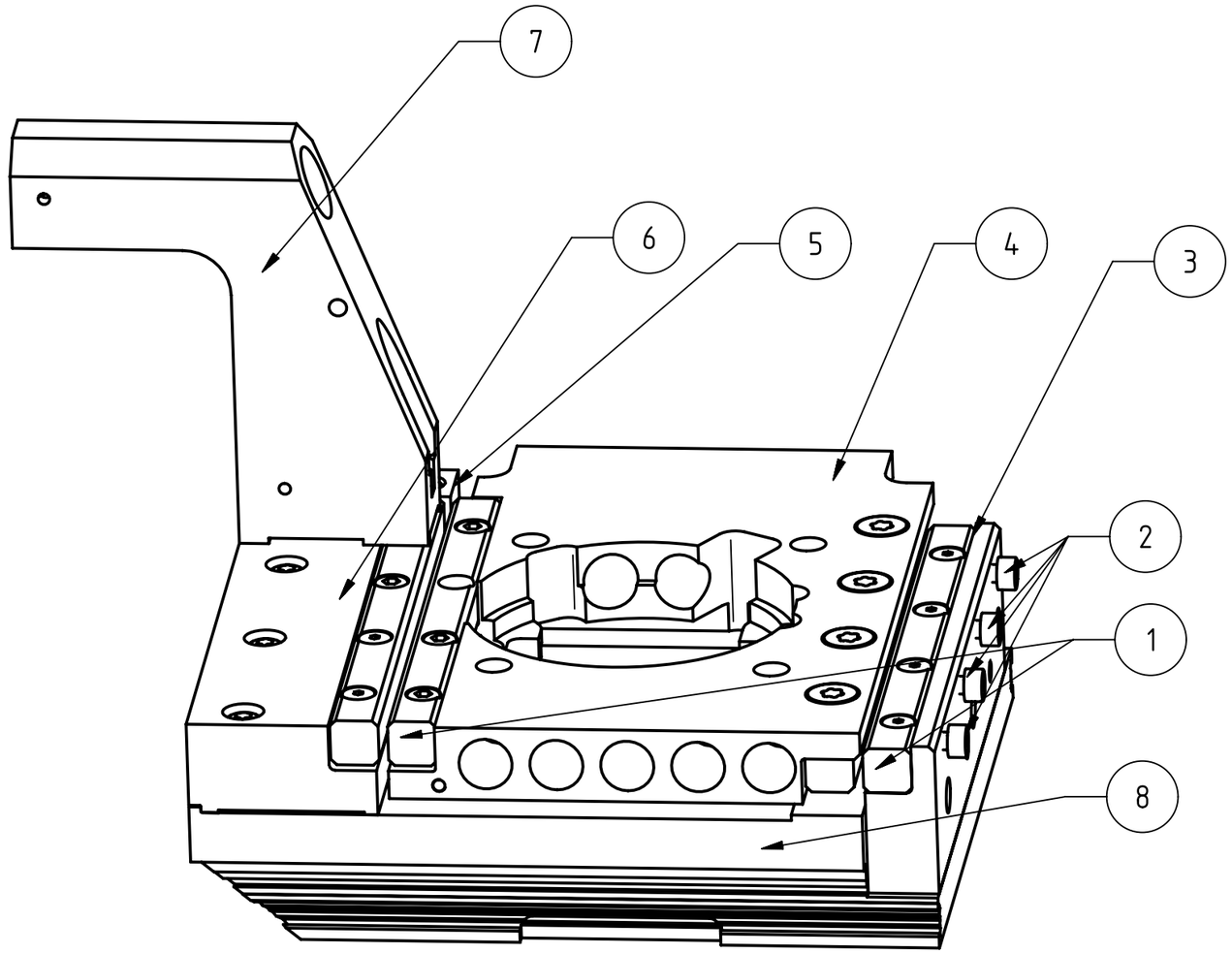

POS	NC	N	NAME	NOTE
9				
8	1023175	1	X SLIDE	CD-DRAW\GUIDE\1023175
7	1024379	1	BLOCK X DRIVE	CD-DRAW\GUIDE\1024349
6	1023188	1	Y GUIDE	CD-DRAW\GUIDE\1023188
5	1023677	1	STOP BLOCK	CD-DRAW\GUIDE\1023677
4	1023182	1	Y SLIDE	CD-DRAW\GUIDE\1023182
3	1023173	1	BLOCK Y GUIDE	CD-DRAW\GUIDE\1023173
2		4	ADJU, SCR	M3
1		2	LINEAR GUIDE	LWR3100

THIRD ANGLE PROJECTION

FEI™

PREDECESSOR: | REVISION:

STATUS:

GENERAL ROUGHNESS: $\sqrt{}$ Ra in µm

MATERIAL:

NAME: Vaske, Frantisek

SCALE: NTS

TREATMENT:

SHEET BIRTH DATE: 21-May-2012

SIZE: A3

UNIT: mm

TITLE: lwr3100

PART NUMBER: 1023134 | REVISION: A

DRAWN ACCORDING TO: QEO-11-010

FILE TYPE: ☑ | LOCATION: BRNO | SHEET NAME: Physical data

SHEET 110-01 OF 01

REV	DATE	ECR	DESCRIPTION OF CHANGE	NAME
A	22-May-2012			Vaske, Frantisek

ATTACHMENT 4

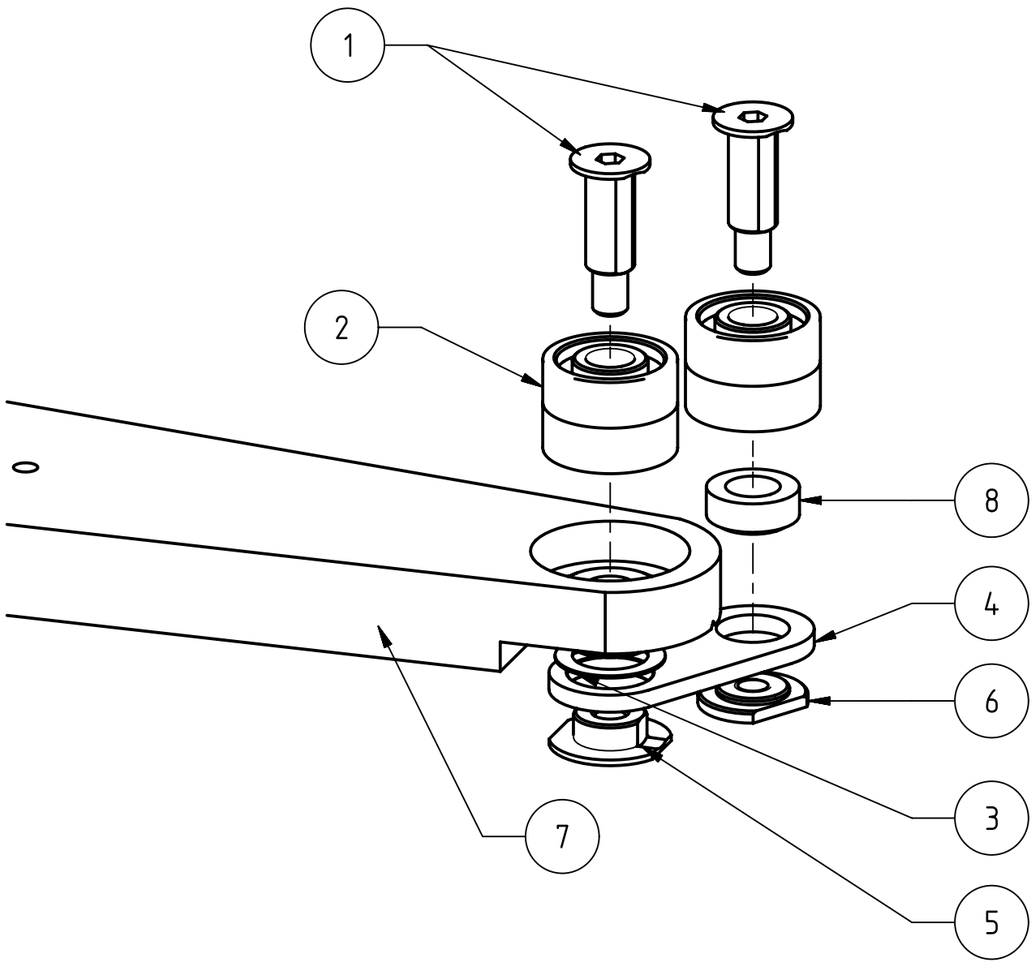

9				
8	1016399	1	SP. INSERT	CD-DRAW\PULL\1016399
7	4022 197 74784	1	ARM	
6	1016409	1	FIX NUT	
5	4022 197 734443	1	SUBARM NUT	
4	1016361	1	SUBARM	CD-DRAW\PULL\1016361
3	4022 260 13141	1	WASHER	
2	4022 198 19761	2	PAIR BEARING	4x11x4
1	4022 197 73462	2	SUBARM SCREW	
POS	NC	N	NAME	NOTE

THIRD ANGLE PROJECTION

FEI™

PREDECESSOR: | REVISION:

STATUS:

GENERAL ROUGHNESS: – / Ra in µm

MATERIAL:

NAME: Vaske, Frantisek

SCALE: NTS

TREATMENT:

SHEET BIRTH DATE: 22-May-2012

SIZE: A3

UNIT: mm

TITLE: SNUB PULLEY ASSEMBLY

PART NUMBER: 1016365 | REVISION: A

DRAWN ACCORDING TO: QEO-11-010

FILE TYPE: ☑ | LOCATION: BRNO | SHEET NAME: Physical data

SHEET 110-01 OF 01

Attachment 5

Stage kinematic chain